UC Irvine
UC Irvine Previously Published Works

Title

Prospects for indirect detection of neutralino dark matter

Permalink

https://escholarship.org/uc/item/7134s4s6

Journal

Physical Review D, 63(4)

ISSN

2470-0010

Authors

Feng, Jonathan L
Matchev, Konstantin T
Wilczek, Frank

Publication Date

2001-02-15

DOI

10.1103/physrevd.63.045024

Peer reviewed

Prospects for indirect detection of neutralino dark matter

Jonathan L. Feng,[1] Konstantin T. Matchev,[2] and Frank Wilczek[1]

[1]*School of Natural Sciences, Institute for Advanced Study, Princeton, New Jersey 08540*
[2]*Theoretical Physics Department, Fermi National Accelerator Laboratory, Batavia, Illinois 60510*

Dark matter candidates arising in models of particle physics incorporating weak scale supersymmetry may produce detectable signals through their annihilation into neutrinos, photons, or positrons. A large number of relevant experiments are planned or underway. The ''logically possible'' parameter space is unwieldy. By working in the framework of minimal supergravity, we can survey the implications of the experiments for each other, as well as for direct searches, collider searches, low-energy experiments, and naturalness in a transparent fashion. We find that a wide variety of experiments provide interesting probes. Particularly promising signals arise in the mixed gaugino-Higgsino region. This region is favored by low-energy particle physics constraints and arises naturally from minimal supergravity due to the focus point mechanism. Indirect dark matter searches and traditional particle searches are highly complementary. In cosmologically preferred models, if there are charged superpartners with masses below 250 GeV, then some signature of supersymmetry must appear *before* the CERN LHC begins operation.

I. INTRODUCTION

It is now well established that luminous matter makes up only a small fraction of the mass of the observed universe. The evidence for dark matter is both astrophysical and cosmological [1]. Such evidence requires only that dark matter is gravitationally interacting. However, additional constraints, especially the success of light-element cosmonucleosynthesis calculations, strongly disfavor the possibility that dark matter is composed solely of baryons [2], and so some form of matter foreign to our everyday world is required. The dark matter problem is therefore also an important problem for particle physics, as particle physics both suggests promising possibilities and imposes stringent constraints.

Neutralinos are well-motivated candidates to provide much or all of the non-baryonic dark matter. An effectively stable particle is a generic component of models with weak-scale supersymmetry. This particle is the lightest supersymmetric particle (LSP), and is typically the neutralino, a mixture of the superpartners of Higgs and electroweak gauge bosons. Particle physics considerations alone require the neutralino to be electrically neutral, effectively stable (assuming R-parity conservation, which is also motivated by the need to forbid too-rapid proton decay), and weakly interacting, with mass of order 100 GeV (required, as we shall quantify below, if supersymmetry naturally protects the electroweak scale from large radiative corrections). Remarkably, these properties are consistent with the possibility that the thermal relic density of neutralinos makes up most of the missing mass of the universe [3,4].

Unfortunately, these properties also guarantee that neutralinos are practically impossible to observe in collider experiments directly. They pass through collider detectors without interacting. Existing bounds on neutralinos therefore rely on model-dependent correlations between their properties and those of other supersymmetric particles. At present, in minimal supergravity, the CERN e^+e^- collider LEP experiments constrain $m_\chi \gtrsim 40$ GeV [5]. In the next several

years, run II of the Tevatron at Fermilab and, eventually, the Large Hadron Collider (LHC) at CERN will provide more powerful collider probes.

If neutralinos make up a significant portion of the halo dark matter, many additional avenues for their detection open up. They may deposit energy as they scatter off nuclei in detectors. We have investigated the prospects for direct detection in a companion article [6], where we emphasized the importance and promise of a mixed gaugino-Higgsino regime, previously neglected. Here we will study the possibility of detecting neutralinos indirectly by looking for evidence of their annihilation [7]. In the next five years, an astounding array of experiments will be sensitive to the various potential neutralino annihilation products. These include under-ice and underwater neutrino telescopes (AMANDA, NESTOR, ANTARES), atmospheric Cherenkov telescopes (STACEE, CELESTE, ARGO-YBJ, MAGIC, HESS, CANGAROO, VERITAS), space-based γ ray detectors (AGILE, AMS/γ, GLAST), and antimatter-antiparticle experiments (PAMELA, AMS). In many cases, these experiments will improve current sensitivities by several orders of magnitude.

In this paper we evaluate the prospects for neutralino dark matter discovery through indirect detection. The neutralino signals depend on many unknown parameters. At the same time, an abundance of theoretical and experimental information from particle physics can be brought to bear. The implications of traditional particle physics searches for dark matter searches, and *vice versa*, are already significant, and promise to become much stronger over the next few years. One of our main conclusions is that in a class of particle physics models favored by current particle physics constraints, astrophysical signals are especially enhanced.

Previous discussions of indirect neutralino detection fall rather sharply into two schools. Several previous works are based on specific high energy models [8,9], including a number in the framework of minimal supergravity [10–14]. As we will recall below, minimal supergravity incorporates several desirable features, including the radiative breaking of electroweak symmetry and the possibility, suggested by gauge coupling unification [15], of perturbative extrapolation

to large energy scales. Previous studies in minimal super-gravity have concluded that only *B*-ino-like dark matter is allowed by particle physics constraints. Such dark matter necessarily implies highly suppressed dark matter signals, as we will see. These studies, and their somber conclusions, have been criticized as products of overly restrictive particle physics assumptions [16]. Recently we have argued more specifically that, even in minimal models, these studies failed to examine a very well-motivated regime of parameters, and that for this reason their conclusions are overly pessimistic [6].

At the other extreme, several studies scan over a large set of weak-scale supersymmetry parameters and consider values for these parameters as large as 50 TeV. (See, for example, Refs. [16–20].) These studies, and others, bring a high level of sophistication to the evaluation of astrophysical effects on dark matter signals. In this regard, we will have nothing to add, but we will incorporate many of the most accurate recent results in our study.

From a particle physics perspective, this second group of studies is impressively general, but this generality is achieved at a cost. For example, extrapolating a given set of weak-scale parameters to higher scales, one may encounter such diseases as Landau poles or charge- or color-breaking minima. Models of this sort do not arise within a reasonable high energy framework. In addition, there is the practical difficulty that the proliferation of free parameters implies that results cannot be presented in a systematic, yet transparent, fashion. Typically they are displayed as scatter plots after scanning over all parameters. It is nearly impossible, from such plots, to determine the dependence of the signal rates on the underlying physical parameters. Dedicated correlation plots have been used to highlight a few of the relations between dark matter detection experiments, but even the most general implications of these experiments for collider searches, electric dipole moments, anomalous magnetic moments, proton decay, flavor violation, and other searches for supersymmetry are very hard to discern. Finally, it can be expected that super-symmetry parameters, such as the μ and gaugino mass parameters, of order 50 TeV will require fine-tuning of the order of 1 part in 10^6 to produce the observed electroweak scale. (While it is impossible to speak of naturalness without first specifying a mechanism of electroweak symmetry breaking, at present all concrete models display this feature.) Such large fine-tuning destroys one of the main motivations for considering supersymmetric extensions of the standard model in the first place. Lacking both a systematic framework and a systematic presentation, it is impossible to see how the expectations narrow when some naturalness criterion is imposed.

It may be impossible to satisfy both schools simultaneously. However, recent results suggest an appealing compromise. As has been emphasized in Refs. [21–23], a *B*-ino-like LSP is *not* a robust prediction of minimal supergravity. We find that both *B*-ino-like and mixed gaugino-Higgsino dark matter is possible. So simply by considering all of minimal supergravity parameter space carefully, as we will do here, we remove the most egregious form of model dependence. At the same time, by staying within the confines of minimal supergravity we will be able to present results in an organized and comprehensive manner, so that correlations with all other supersymmetric signals are easily determined. As the experiments discussed below report results, it will be ever more interesting to see what models are being excluded or favored. The framework discussed here makes this possible.

Inclusion of the new gaugino-Higgsino LSP models in minimal supergravity is not just a formality. The region with mixed gaugino-Higgsino LSPs is now known to be robust and natural, given an objective definition of naturalness [21–23]. It yields cosmologically interesting relic densities [6], and is even favored by low energy constraints such as proton decay and electric dipole moments [24]. As we will see, *all* indirect detection signals are enhanced in this region. This lends increased interest to indirect dark matter searches, since large—possibly spectacular—rates are predicted within an attractive and simple high energy framework.

In the following section, we review a few essential results concerning neutralino dark matter in minimal supergravity with an emphasis on the new gaugino-Higgsino LSP region. We then consider each of three promising signals in the following sections: upward-going muons from neutrinos in Sec. III, photons in Sec. IV, and positrons in Sec. V. In Sec. VI we compare these to direct dark matter and traditional particle physics searches, and in Sec. VII we summarize our results.

II. NEUTRALINO DARK MATTER AND ITS ANNIHILATION

The lightest neutralino is the LSP in many supersymmetric models. Assuming *R*-parity conservation to prevent too-rapid proton decay through dimension-four operators, the LSP is effectively stable, and the neutralino is then an excellent candidate for cold dark matter.

The signals of neutralino dark matter are determined in large part by their composition. Neutralinos are mixtures of the superpartners of Higgs and electroweak gauge bosons. After electroweak symmetry breaking, these gauge eigenstates mix through the tree-level mass matrix

$$\begin{pmatrix} M_1 & 0 & -m_Z \cos\beta \sin\theta_W & m_Z \sin\beta \sin\theta_W \\ 0 & M_2 & m_Z \cos\beta \cos\theta_W & -m_Z \sin\beta \cos\theta_W \\ -m_Z \cos\beta \sin\theta_W & m_Z \cos\beta \cos\theta_W & 0 & -\mu \\ m_Z \sin\beta \sin\theta_W & -m_Z \sin\beta \cos\theta_W & -\mu & 0 \end{pmatrix} \qquad (1)$$

in the basis $(-i\widetilde{B}, -i\widetilde{W}^3, \widetilde{H}_u^0, \widetilde{H}_d^0)$. The weak scale parameters entering this mass matrix are the B-ino, W-ino, and Higgsino mass parameters M_1, M_2, and μ, and the ratio of Higgs scalar vacuum expectation values $\tan\beta = \langle H_u^0 \rangle / \langle H_d^0 \rangle$. The lightest neutralino mass eigenstate is then determined by these parameters to be some mixture

$$\chi \equiv \chi_1^0 = a_1(-i\widetilde{B}) + a_2(-i\widetilde{W}^3) + a_3\widetilde{H}_u^0 + a_4\widetilde{H}_d^0. \quad (2)$$

We define the LSP gaugino fraction to be

$$R_\chi \equiv |a_1|^2 + |a_2|^2. \quad (3)$$

In the following, we refer to neutralinos with $0.9 < R_\chi$ as gaugino-like, $0.1 \leq R_\chi \leq 0.9$ as mixed gaugino-Higgsino, and $R_\chi < 0.1$ as Higgsino-like.

The preceding discussion is model-independent, assuming only minimal field content. However, the minimal supersymmetric standard model is undoubtedly a low-energy effective theory of a more fundamental theory defined at some higher scale, such as the grand unified theory (GUT) or string scale. A simple realization of this idea is the framework of minimal supergravity, which is fully specified by the five parameters (four continuous, one binary)

$$m_0, M_{1/2}, A_0, \tan\beta, \text{sgn}(\mu). \quad (4)$$

Here, m_0, $M_{1/2}$, and A_0 are the universal scalar mass, gaugino mass, and trilinear scalar coupling. They are assumed to arise through supersymmetry breaking in a hidden sector at the GUT scale $M_{\text{GUT}} \simeq 2 \times 10^{16}$ GeV. The hidden-sector parameters then determine all the couplings and masses of the weak scale Lagrangian through renormalization group evolution. In particular, electroweak symmetry is broken radiatively by the effects of a large top quark Yukawa coupling, and the electroweak scale is determined in terms of supersymmetry parameters through

$$\frac{1}{2}m_Z^2 = \frac{m_{H_d}^2 - m_{H_u}^2 \tan^2\beta}{\tan^2\beta - 1} - \mu^2. \quad (5)$$

Equation (5) receives corrections beyond tree level; in our work we include all one-loop effects in the Higgs potential [25]. We also use two-loop renormalization group equations [26] with one-loop threshold corrections [25,27] and calculate all superpartner masses to one-loop [25]. All of the qualitative features to be described below are present, however, also for one-loop renormalization group equations.

Minimal supergravity is, of course, by no means the most general allowed framework. It is worth noting, however, that the assumptions most relevant for dark matter, namely, the universality of gaugino and scalar masses, are motivated not only by their simplicity, but also by concrete experimental facts. The case for gaugino mass unification is especially powerful. In the minimal supersymmetric standard model, the three gauge couplings, when evolved to high scales, meet with high precision at a point, the GUT scale [15]. If the standard model is unified in a grand unified gauge theory, one typically obtains also gaugino mass unification. The uni-

fication of couplings calculation also distinguishes $M_{\text{GUT}} \simeq 2 \times 10^{16}$ GeV as the natural scale for a more fundamental framework.

The unification of scalar masses is motivated by a similar, although more speculative, argument. Consider the mass parameter $m_{H_u}^2$, which, from Eq. (5), plays the critical role in determining the weak scale for all moderate and large values of $\tan\beta$ ($\tan\beta \gtrsim 5$). For theories with a universal scalar mass, it is a remarkable fact that the renormalization group trajectories of $m_{H_u}^2$ for various initial conditions m_0, when evolved to low scales, meet with high precision at a point, the weak scale [21,22]. This focusing, which requires that the top quark mass be within ~ 5 GeV of its measured value, implies that the electroweak potential is highly insensitive to m_0. The longstanding problems of supersymmetry with respect to CP violation, proton decay, etc. can therefore be ameliorated without fine-tuning, simply by assuming large scalar masses. Although the focusing property holds more generally, its minimal and most concrete realization is in theories with a universal scalar mass. The assumption of a universal (and large) scalar mass is therefore motivated by the fact that it provides a simple and elegant solution to several well-known phenomenological problems of weak scale supersymmetry.

Given these motivations for minimal supergravity, we now consider their implications for neutralino dark matter. Gaugino mass unification implies $M_1 \simeq M_2/2 \simeq 0.4 M_{1/2}$. Dark matter is therefore never W-ino-like,[1] and in fact, throughout parameter space, $|a_2|^2 < 0.07$. Additional insights follow from re-writing Eq. (5) in terms of GUT scale parameters. For $A_0 = 0$ and $\tan\beta = 10$, for example,

$$\frac{1}{2}m_Z^2 \approx -0.04m_0^2 + 1.4M_{1/2}^2 - \mu^2, \quad (6)$$

where the numerical coefficients of the first two terms vary fractionally by $\mathcal{O}(10\%)$ in the $(m_0, M_{1/2})$ plane [21,22]. The coefficient of m_0^2 is highly suppressed [30,31]. This is another expression of the focusing behavior discussed above, and implies that multi-TeV values of m_0 do not involve significant large fine-tuning. The coefficient is also negative. For fixed $M_{1/2}$, as m_0 increases, $|\mu|$ decreases, and the LSP becomes increasingly Higgsino-like. This is important, because even a 10% Higgsino admixture drastically affects the phenomenology. In Figs. 1 and 2 we show the LSP mass and gaugino fraction in the $(m_0, M_{1/2})$ plane. For large $m_0 \gtrsim 1$ TeV, we find a region, previously ignored, where the LSP has a significant Higgsino component. The green shaded regions are excluded by the requirement that the LSP be neutral (top left) and by the chargino mass limit of 95 GeV (bottom and right).

---

[1] W-ino-like LSPs exist in other frameworks, but typically they annihilate far too quickly to be cosmologically relevant [28]. Interesting relic densities are possible, however, if there is some mechanism of late production [29].
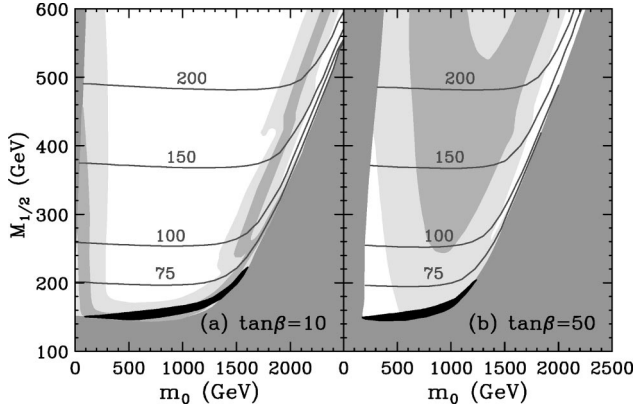
FIG. 1. Contours of constant LSP mass m_χ in GeV in the $(m_0, M_{1/2})$ plane for $A_0=0$, $\mu>0$, $m_t=174$ GeV, and two representative values of $\tan\beta$. The green shaded regions are excluded by the requirement that the LSP be neutral (left) and by the chargino mass limit of 95 GeV (bottom and right). We have also delineated the regions with potentially interesting values of the LSP relic abundance: $0.025\leq\Omega_\chi h^2\leq1$ (yellow) and $0.1\leq\Omega_\chi h^2\leq0.3$ (light blue). In the black region, $|2m_\chi-m_h|<5$ GeV, and neutralino annihilation is enhanced by a Higgs resonance.

In Figs. 1 and 2, we also indicate the regions of cosmologically interesting relic densities; see Ref. [6] for details. A generous range is $0.025\leq\Omega_\chi h^2\leq1$, where the lower bound is the requirement that neutralino dark matter explain galactic rotation curves and the upper bound follows from the lifetime of the universe. Above this shaded region, $\Omega h^2>1$; below, $\Omega h^2<0.025$. The range $0.1\leq\Omega_\chi h^2\leq0.3$ is most preferred by current limits. Our relic density calculation is not trustworthy in the black region, where there is a Higgs scalar resonance, and very near to the left and right borders of the excluded region, where co-annihilation is important [32–35]. In the bulk of parameter space, however, these effects are negligible. For all $\tan\beta$, cosmologically interesting densities are possible for $m_0\gtrsim1$ TeV. For $\tan\beta=10$, the cosmologically preferred region contains gaugino-Higgsino dark matter.

In contrast to m_0, the parameters $M_{1/2}$ and μ enter Eq. (6) with $\mathcal{O}(1)$ coefficients. Naturalness therefore requires that the LSP mass (and, in fact, the masses of all four neutralinos and both charginos) should not be too far above the electroweak scale. While in principle it is possible that in some fundamental framework $M_{1/2}$ and μ are correlated precisely in a way that allows both parameters to be large without fine-tuning (a possibility considered in Ref. [36]), no such framework has been found to date. Barring such a possibility, extreme values such as $M_{1/2}, \mu\sim50$ TeV require a fine-tuning of 1 part in 10^6 and destroy one of the prime motivations for weak-scale supersymmetry. We therefore regard such large values as highly disfavored, and we will focus on neutralino masses of order 100 GeV.

Neutralinos annihilate through a variety of channels. The three leading processes are shown in Fig. 3. (Note that co-annihilation, while potentially important in determining relic densities in the early universe, is negligible now.) Annihilation into gauge bosons is of particular importance, as these
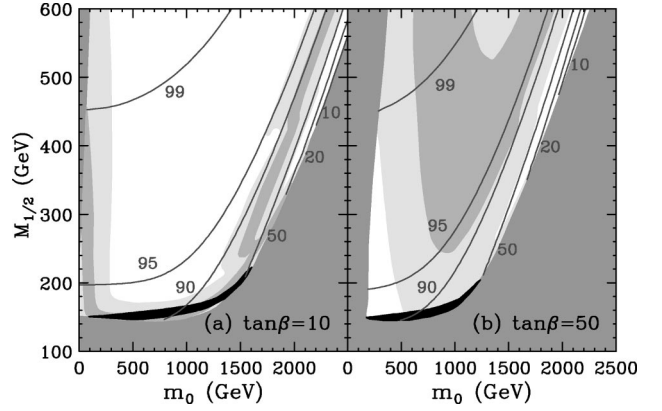

FIG. 2. Contours of constant gaugino fraction R_χ in percent, for the same values of the parameters as in Fig. 1.

processes lead to more energetic and striking signals. The WW cross section relies on $W\chi\chi_i^\pm$ interactions. The only such couplings allowed by gauge invariance are $W\tilde{H}^0\tilde{H}^\pm$ and $W\tilde{W}^0\tilde{W}^\pm$. However, as noted above, gaugino mass unification implies that the W-ino content of the LSP is always negligible. A large WW cross section is therefore possible only when the LSP has a significant Higgsino component. The same conclusion holds for the ZZ process, where the $Z\chi\chi_i^0$ interaction is possible only through $Z\tilde{H}^0\tilde{H}^0$ couplings. In Fig. 4, we see that the annihilation cross sections for $\chi\chi\to WW$ and $\chi\chi\to ZZ$ are indeed highly suppressed in regions with B-ino-like LSPs, but are enhanced by three to four orders of magnitude in regions with mixed gaugino-Higgsino dark matter. As we will see, this region, favored by low energy constraints, will be the most promising for all indirect signals.

Before closing this section, we note several features of Figs. 1 and 2 that will also apply to many of the following figures. Unless otherwise noted, we present results for $A_0=0$, $\mu>0$, $m_t=174$ GeV, and representative values of $\tan\beta$ as indicated. A_0 governs the left-right mixing of scalars, and does not enter the neutralino sector. It is therefore largely irrelevant, especially in the regions of parameter space with observable signals—where, as we will see, the scalars are heavy and decoupled.[2] (In addition, the most important trilinear coupling, A_t, has a weak-scale fixed point, and so is only weakly sensitive to A_0.) Our dark matter results are rather insensitive to the sign of μ, but the choice $\mu>0$ is motivated by the constraint from $B\to X_s\gamma$ (see, e.g. [37]). Finally, perturbativity of Yukawa couplings limits $\tan\beta$ to

---

[2]For $A_0=0$, the 1999 LEP bound on the mass of the lightest CP-even Higgs boson $m_h>107.7$ GeV barely constrains the parameter space shown in our figures, while the 2000 limit $m_h>113.3$ GeV excludes the region with $m_0\lesssim1$ TeV and $M_{1/2}\lesssim300$ GeV. However, the Higgs search is highly sensitive to the A_0 parameter. For other values of A_0, the current constraints may be evaded with negligible impact on our predictions for indirect dark matter detection. For this reason, we do not include the Higgs boson mass constraints in the following analysis.
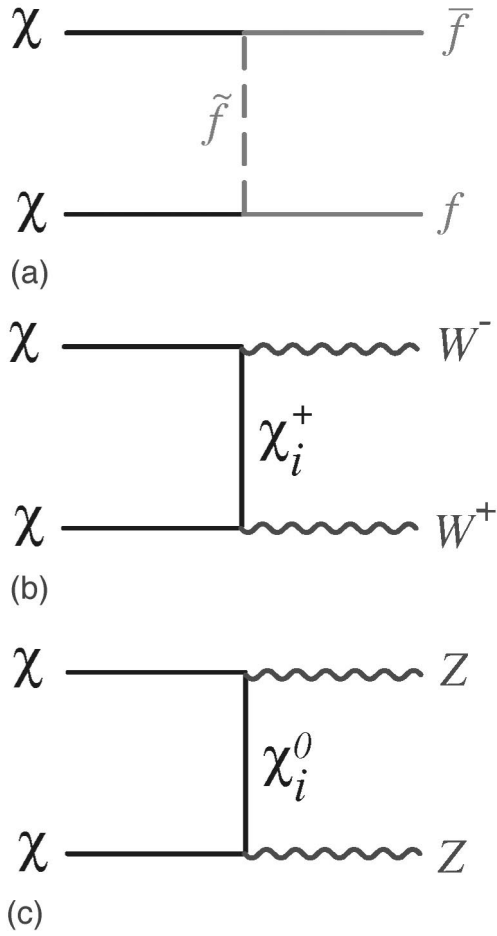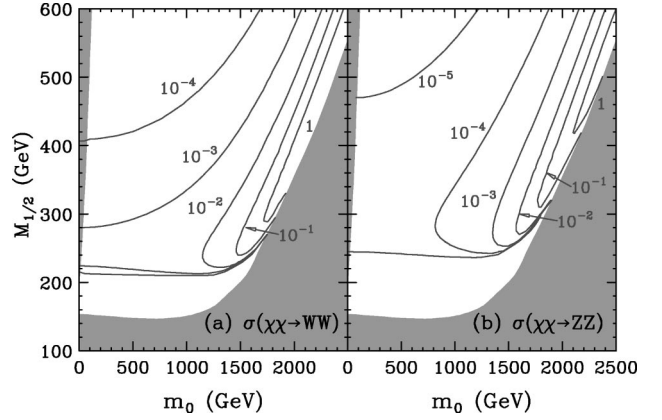
(a)

(b)

(c)

FIG. 3. Three leading neutralino annihilation channels.

FIG. 4. Contours of constant σv in pb for (a) $\chi\chi \to WW$ and (b) $\chi\chi \to ZZ$. We fix $A_0 = 0$, $\mu > 0$, $m_t = 174$ GeV, and $\tan\beta = 10$.

the range $1 \lesssim \tan\beta \lesssim 60$. Low values of $\tan\beta \lesssim 3$ are now being excluded by the LEP Higgs search. In the remaining interval, models with moderate and high values may have qualitatively different behavior, as processes proportional to down-type Yukawa couplings are enhanced by $\tan\beta$. We therefore typically present results for two representative values, one in each range. Plots of many other quantities, including all physical slepton, squark, and Higgs boson masses in the $(m_0, M_{1/2})$ plane, including the high m_0 region, may be found in Refs. [21–23].

Finally, in the following three sections, we will *not* include the effects of variations in thermal relic density in our signal rates, but rather assume, for concreteness, a fixed local neutralino density. The results are then more transparent, and are applicable to general scenarios, such as those in which a late source of neutralino production is present. Of course, in the simplest scenario, models with $\Omega_\chi h^2 > 1$ are excluded, and those with an under-abundance of neutralinos are disfavored and imply suppressed or negligible dark matter signals. This should be kept in mind in the following sections. In Secs. VI and VII, we will combine all these considerations, and focus on the most preferred regions.

III. NEUTRINOS

When neutralinos pass through astrophysical objects, they may be slowed below escape velocity by elastic scattering.

Once captured, they then settle to the center, where their densities and annihilation rates are greatly enhanced. While most of their annihilation products are immediately absorbed, neutrinos are not. High energy neutrinos from the cores of the Earth [38–41] and Sun [40,42–47] are therefore promising signals for indirect dark matter detection.

The formalism for calculating neutrino fluxes from dark matter annihilation is well developed. (See Ref. [48] for a review.) The neutrino flux depends first and foremost on the neutralino density, which is governed by the competing processes of gravitational capture and neutralino annihilation. If N is the number of neutralinos in the Earth or Sun, $\dot{N} = C - AN^2$, where C is the capture rate and A is the total annihilation cross section times relative velocity per volume. The present neutralino annihilation rate is then

$$\Gamma_A = \frac{1}{2}AN^2 = \frac{1}{2}C\tanh^2(\sqrt{CA}\, t_\odot), \qquad (7)$$

where $t_\odot \approx 4.5$ Gyr is the age of the solar system.

Captured neutralinos then annihilate through the processes of Fig. 3. As $\chi\chi \to f\bar{f}$ is helicity-suppressed, neutrinos are produced only in the decays of primary annihilation
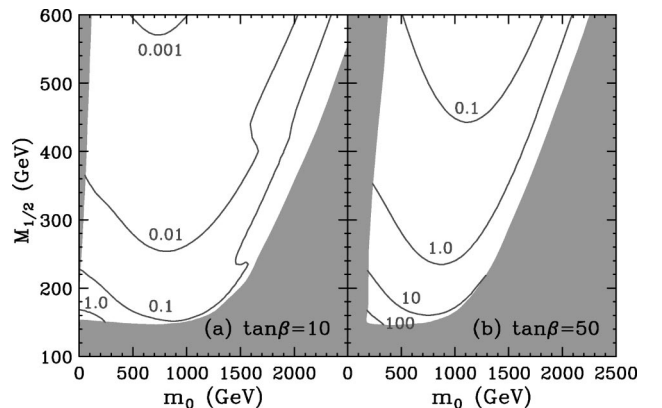
FIG. 5. The filling parameter $\sqrt{CA}\, t_\odot$ for the Earth. We assume neutralino velocity dispersion $\bar{v} = 270$ km/s and a local density of $\rho_0 = 0.3$ GeV/cm^3.
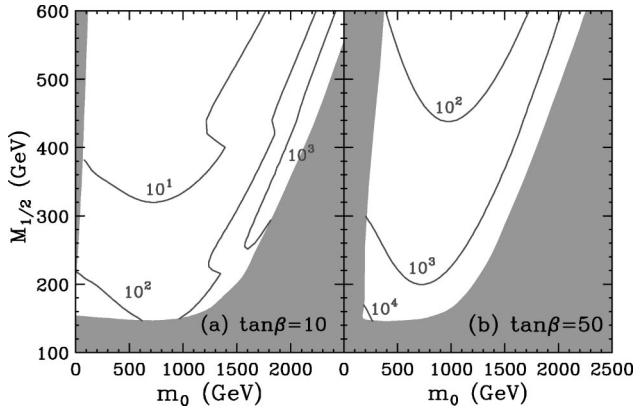
FIG. 6. As in Fig. 5, but for the Sun.

FIG. 7. The capture rate of neutralinos C in s^{-1} in the center of the Earth (for $\bar{v} = 270$ km/s and $\rho_0 = 0.3$ GeV/cm^3).
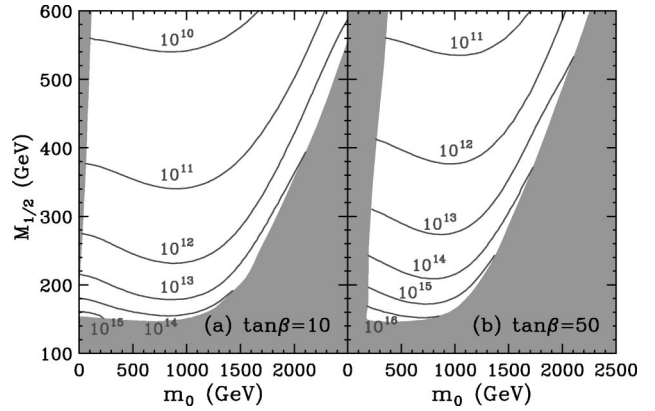
products. Typical neutrino energies are then $E_\nu \sim \frac{1}{2} m_\chi$ to $\frac{1}{3} m_\chi$, with the most energetic spectra resulting from WW, ZZ, and, to a lesser extent, $\tau\bar{\tau}$. After propagating to the Earth's surface, neutrinos are detected through their charged-current interactions. The most promising signal is from upward-going muon neutrinos that convert to muons in the surrounding rock, water, or ice, producing through-going muons in detectors. The detection rate for such neutrinos is greatly enhanced for high energy neutrinos, as both the charged-current cross section and the muon range are proportional to E_ν.

The calculation of muon fluxes from neutralino annihilation in the Earth and Sun is on reasonably firm footing, as it depends only on the local dark matter density and is insensitive to details of halo modeling.[3] Nevertheless, the calculation is involved, primarily as a result of complications in evaluating capture rates [51–53] and, in the case of the Sun, in propagating the neutrinos from the core to the surface [40,54,55]. Here we make use of the procedure of Refs. [48,56]. For other analyses, see Refs. [57–59,17], as well as those motivated by the Tevatron $e^+e^-\gamma\gamma$ event [60,61] and by the DAMA annual modulation signal [62,63].

The ''filling parameters'' $\sqrt{CA}\, t_\odot$ for the Earth and Sun are given in Figs. 5 and 6. For the Sun, $\sqrt{CA}\, t_\odot \gg 1$ for all supersymmetry parameters. The neutralino density has therefore reached equilibrium, and the annihilation rate is at full strength, with $\Gamma_A \approx C/2$. For the Earth, however, typically $\sqrt{CA}\, t_\odot \ll 1$, and the annihilation rate is $\Gamma_A \approx \frac{1}{2} C^2 A\, t_\odot^2$ and far from maximal. As we will see, this plays an important part in reducing the Earth's signal below the Sun's.

The other major ingredient in the muon flux computation is the estimate of the neutralino capture rate C, which is shown in Figs. 7 and 8 for the Earth and Sun, respectively. The elemental compositions of the Earth and Sun are given in Ref. [11]. A quick comparison of Figs. 7 and 8 reveals

that, not surprisingly, a large astrophysical body like the Sun is much more efficient in trapping neutralinos. The Earth's capture rate is, however, enhanced by the iron resonance for very light neutralino masses $m_\chi \sim 50$ GeV. The $\tan\beta$ dependence is also noteworthy. The capture rate in the Earth is determined primarily by the spin-independent elastic scattering cross section for $\chi q \to \chi q$ through s-channel squarks and t-channel Higgs boson exchange. All amplitudes require chirality flips, either through Higgs interactions, squark mass insertions, or quark mass insertions. The first two are proportional to $\tan\beta$ and therefore dominate for moderate and large $\tan\beta$, leading to $C \sim \tan^2\beta$. In contrast, for the Sun, the $\tan\beta$ dependence is minimal; the dominant contribution is from axial-vector scattering off hydrogen, which is largely independent of $\tan\beta$.

Muon flux rates from the Earth and Sun are presented in Figs. 9 and 10. Consistent with previous studies (see, e.g. [14]), we find that the flux rate is indeed small in regions of parameter space with $m_0 < 1$ TeV and B-ino-like LSPs. However, for $m_0 > 1$ TeV, in the region where $m_\chi > m_W$ and the dark matter is a gaugino-Higgsino mixture, the fluxes are greatly enhanced. Here, annihilation to gauge bosons is unsuppressed, resulting in a hard neutrino spectrum and large muon fluxes. In this region, the rates from the Sun are large for all values of $\tan\beta$. For the Earth, we see that, despite the close proximity of the Earth's center, the muon fluxes are

---

[3]It has been suggested that muon fluxes may be enhanced, by up to two orders of magnitude, due to capture of neutralinos in highly eccentric solar system orbits [49]. The magnitude of the enhancement depends on details of the neutralino parameters and involves astrophysical issues still under debate [50]. We have not included it here.
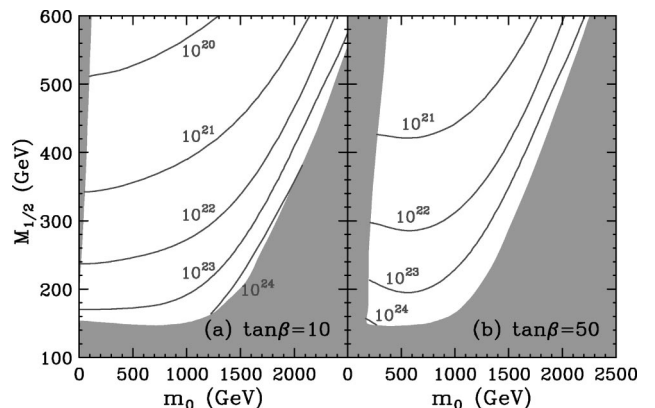

FIG. 8. Same as in Fig. 7, but for the Sun.
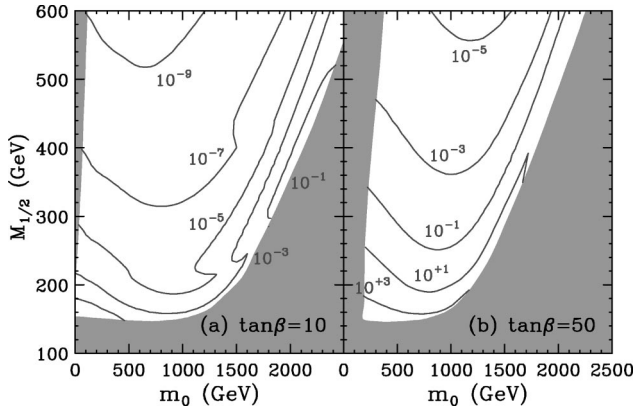
FIG. 9. Muon flux from the Earth in km^{-2} yr^{-1} (for $\bar{v} = 270$ km/s and $\rho_0 = 0.3$ GeV/cm^3).

FIG. 10. As in Fig. 9, but for the Sun.

typically suppressed by several orders of magnitude relative to those from the Sun. However, reasonably large rates are possible even for the Earth for large $\tan\beta$, and particularly for very light neutralinos, where the capture rate is enhanced by the iron resonance, as discussed above.

The theoretical predictions of Figs. 9 and 10 can be compared with the experimental sensitivities of ongoing and near future detectors [64]. These experiments, along with their more salient characteristics and flux limits (where available), are listed in Table I. The flux limits depend on the expected angular dispersion in the signal. This dispersion has two possible origins. One is the source: although neutralinos from the Sun are essentially a point source, in the Earth, 98% of neutralino annihilations occur within a cone of half-angle $8.6° \sqrt{50 \text{ GeV}/m_\chi}$ [52,53]. The second is the angle $\theta_{rms} \approx 13° \sqrt{25 \text{ GeV}/E_\nu}$ between the neutrino and its daughter muon. As $E_\nu \lesssim m_\chi/2$, θ_{rms} is typically the dominant effect. The flux limits listed are for half-cone sizes of 15°, corresponding roughly to $m_\chi \sim 50$ GeV. Heavier neutralinos will
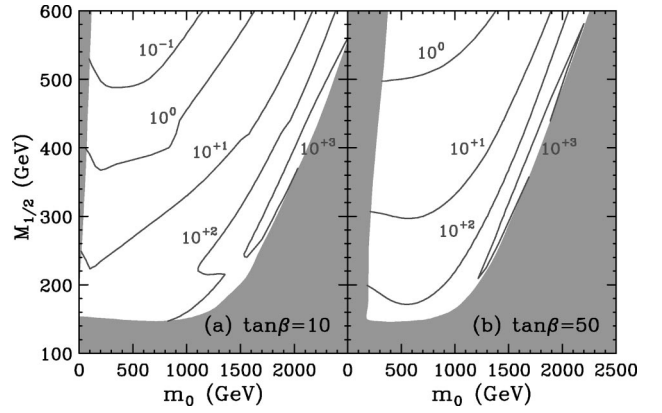
produce more collimated muons, allowing smaller cone sizes with reduced backgrounds. The improved limits for smaller cone sizes may be found in the references.

Comparing Figs. 9 and 10 with Table I, we find that present limits do not significantly constrain the minimal supergravity parameter space. However, given that the effective area of neutrino telescope experiments is expected to increase by 10 to 100 in the next few years, muon fluxes of order 10–100 km^{-2} yr^{-1} may be within reach. Such sensitivities are typically not sufficient to discover B-ino-like LSPs, unless they are light and $\tan\beta$ is large. But they have an excellent opportunity to detect dark matter in the mixed gaugino-Higgsino dark matter scenarios, which, as we have emphasized above, are preferred by low energy particle physics constraints.

Muon energy thresholds, listed in Table I, are not included in Figs. 9 and 10. Since the muon detection rate is dominated by high energy muons as noted above, the threshold energy is typically not important, especially in the regions where a detectable signal is expected. This is not the case for all detectors, however. For example, since muons

TABLE I. Current and planned neutrino experiments. We list also each experiment's (expected) start date, physical dimensions (or approximate effective area), muon threshold energy E_μ^{thr} in GeV, and 90% C.L. flux limits for the Earth $\Phi_\mu^\oplus$ and Sun $\Phi_\mu^\odot$ in km^{-2} yr^{-1} for half-cone angle $\theta \approx 15°$ when available.

Experiment	Type	Date	Dimensions	E_μ^{thr}	$\Phi_\mu^\oplus$	$\Phi_\mu^\odot$
Baksan [65]	Underground	1978	$17\times17\times11$ m^3	1	6.6×10^3	7.6×10^3
Kamiokande [66]	Underground	1983	~150 m^2	3	10×10^3	17×10^3
MACRO [67]	Underground	1989	$12\times77\times9$ m^3	1.5[a]	3.2×10^3	6.5×10^3
Super-Kamiokande [68]	Underground	1996	~1200 m^2	1.6	1.9×10^3	5.0×10^3
Baikal NT-96 [69]	Underwater	1996	~1000 m^2	10	15×10^3	
AMANDA B-10 [70]	Under-ice	1997	~1000 m^{2b}	~25	44×10^{3b}	
Baikal NT-200 [69]	Underwater	1998	~2000 m^2	~10		
AMANDA II [71]	Under-ice	2000	$\sim3\times10^4$ m^2	~50		
NESTOR[c] [72]	Underwater	2000	$\sim10^4$ m^{2d}	few		
ANTARES [73]	Underwater	2003	$\sim2\times10^4$ m^{2d}	$\sim5-10$		
IceCube [71]	Under-ice	2003-8	$\sim10^6$ m^2			

[a]2 GeV for Sun.
[b]Hard spectrum, $m_\chi = 100$ GeV.
[c]One tower.
[d]$E_\mu \sim 100$ GeV.

lose 0.26 GeVper meter in water and ice, neutrino telescopes requiring track lengths of ~ 100 m will have thresholds of order ~ 25 GeV. The dependence on threshold energy has been studied in Refs. [74,18], where it was found that for threshold energies of $E_\mu^{\text{thr}} \sim \frac{1}{4} m_\chi$ to $\frac{1}{6} m_\chi$, the loss of signal is substantial. Low threshold energies in neutrino telescopes are clearly very important for dark matter detection. This conclusion is further strengthened by considerations of naturalness, which favor low neutralino masses.

IV. PHOTONS

High-energy photons provide a unique signal of dark matter annihilation. They point back to their source, and their energy distribution is directly measurable, at least in principle. For these reasons, given sufficient angular and energy resolution in gamma ray detectors, a variety of signals may be considered.

The photon signal may arise from the galactic center [75–77], the galactic halo [78,79], or even from extra-galactic sources [20]. We will consider the galactic center, where large enhancements in dark matter density are possible [19,80]. In contrast to the neutrino signal considered in Sec. III, the photon flux is highly sensitive to halo model parameters. Fortunately, the problem may be separated into two parts: one containing all halo model dependence, and the other all particle physics uncertainties. Given the predicted photon fluxes for a reference halo model, the predictions for all other halo models are then easily determined.

The photon energy distribution receives two types of contributions: line and continuum. The former results from the loop-mediated processes $\chi\chi \to \gamma\gamma$ [81,82] and $\chi\chi \to \gamma Z$ [83]. Because dark matter in the halo is extremely non-relativistic, photons from these processes have an energy width of only $\Delta E_\gamma / E_\gamma \sim 10^{-3}$ and are effectively mono-energetic. While this signal would be the most spectacular of all possible indirect signals, its rates are, of course, suppressed [84]. In a model-independent survey, Bergström, Ullio, and Buckley [19] have found that the photon line may be observable for neutralinos with a large Higgsino component, assuming a cuspy halo profile, such as that of Navarro, Frenk, and White [85], and telescopes with small angular acceptances $\sim 10^{-5}$ sr.

On the other hand, photons may also be produced in the cascade decays of other primary annihilation products. In contrast to the line signal, cascade decays produce a large flux of photons with a continuum of energies. This signal is far less distinctive and will almost certainly require additional confirmation to unambiguously distinguish it from background or other exotic sources. Nevertheless, we will focus here on the continuum signal, as it will provide the first hint of dark matter from gamma ray astronomy.

The differential photon flux along a direction that forms an angle ψ with respect to the direction of the galactic center is

$$\frac{d\Phi_\gamma}{d\Omega dE} = \sum_i \frac{dN_\gamma^i}{dE} \sigma_i v \frac{1}{4\pi m_\chi^2} \int_\psi \rho^2 dl, \qquad (8)$$

where the sum is over all annihilation channels and ρ is the neutralino mass density. All of the halo model dependence is isolated in the integral, which, following Ref. [19], we write in the dimensionless form

$$J(\psi) = \frac{1}{8.5 \text{ kpc}} \left(\frac{1}{0.3 \text{ GeV/cm}^3} \right)^2 \int_\psi \rho^2 dl. \qquad (9)$$

The integral is along the line of sight. Assuming a spherical halo, the mass density is given by $\rho = \rho(r)$, where $r^2 = l^2 + R_0^2 - 2lR_0 \cos\psi$, and $R_0 \approx 8.5$ kpc is the solar distance to the galactic center.

The photon flux is, of course, maximized for $\psi = 0$, but it must be averaged over the field of view. The result is

$$\Phi_\gamma(E_{\text{thr}}) = 5.6 \times 10^{-10} \text{ cm}^{-2}\text{s}^{-1} \times \sum_i \int_{E_{\text{thr}}}^{m_\chi} dE \frac{dN_\gamma^i}{dE} \left(\frac{\sigma_i v}{\text{pb}} \right)$$

$$\times \left(\frac{100 \text{ GeV}}{m_\chi} \right)^2 \bar{J}(\Delta\Omega) \Delta\Omega, \qquad (10)$$

where

$$\bar{J}(\Delta\Omega) \equiv \frac{1}{\Delta\Omega} \int_{\Delta\Omega} J(\psi) \, d\Omega, \qquad (11)$$

and $\Delta\Omega$ is the solid angle of the field of view centered on $\psi = 0$. E_{thr} is the lower threshold energy; detectors also have upper cutoffs, but these are typically irrelevant, as the energy distribution falls steeply with energy. $\bar{J}$ has been studied for a variety of halo models in Ref. [19]. For a typical atmospheric Cherenkov telescope (ACT) acceptance of $\Delta\Omega = 10^{-3}$ sr, the modified isothermal profile described by $\rho(r) \propto [1 + (r/a)^2]^{-1}$ yields $3 \lesssim \bar{J} \lesssim 10^3$. On the other hand, cuspy halos lead to values of $\bar{J}$ as large as 10^5. (Such singular profiles have recently been argued to be incompatible with neutralino dark matter, however, based on radio emission from neutralino annihilation near the black hole at the galactic center [86].) We will choose a moderate reference value $\bar{J}(10^{-3}) = 500$, which is within the allowed ranges of both the modified isothermal and cuspy halos. The factorizability of the photon flux implies that our results can be scaled to all other halo models easily.

The particle physics model dependence enters through all the other factors of Eq. (8). The energy integral is roughly $\int dE \, dN_\gamma^i/dE \sim 0.5$ for all i, but the energy distribution depends significantly on the annihilation channel. The differential gamma ray multiplicity has been simulated for light and heavy neutralinos in Refs. [87] and [19], respectively. The spectrum for the most important annihilation channels is described well by $dN_\gamma/dx = a \, e^{-bx}/x^{1.5}$, where $x \equiv E_\gamma/m_\chi$ and $(a,b) = (0.73, 7.76)$ for WW and ZZ [19], $(1.0, 10.7)$ for $b\bar{b}$, $(1.1, 15.1)$ for $t\bar{t}$, and $(0.95, 6.5)$ for $u\bar{u}$. We neglect Higgs boson final states, as they never have branching fraction greater than 7%. For the gg final state, we use the light quark distribution. Our crude approximation for gluons is relevant only in isolated regions with B-ino-like LSPs where, as we
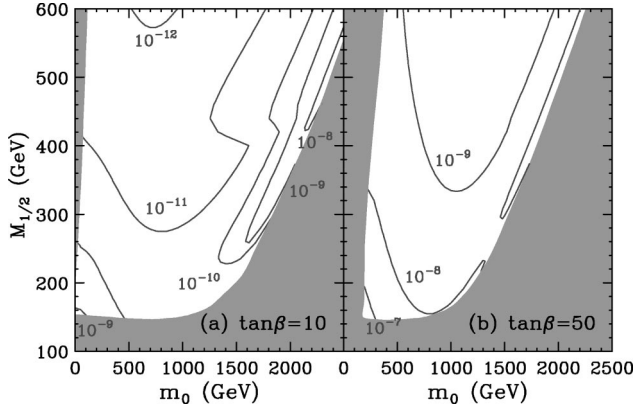
FIG. 11. Photon flux $\Phi_\gamma(E_{thr})$ in cm^{-2} s^{-1} from a 10^{-3} sr cone centered on the galactic center for a threshold energy of $E_{thr}=1$ GeV. We assume halo model parameter $\bar{J}=500$. Results for other halo models may be obtained by scaling to the appropriate $\bar{J}$ (see text).

will see, the signal is unobservable. With the exception of the irrelevant light quark distribution, the WW and ZZ distributions produce the most energetic photons.

The photon flux $\Phi_\gamma(E_{thr})$ is given in Figs. 11–13 for threshold energies of 1, 10 and 50 GeV. The maximal rates are found in the region of parameter space with mixed gaugino-Higgsino dark matter, and are insensitive to $\tan\beta$. Here branching ratios to gauge bosons are large, and the photon spectrum hard. In the rest of parameter space, $b\bar{b}$ is an important final state, and $\Phi_\gamma(E_{thr})$ is enhanced by $\tan\beta$.

In the past, the high energy photon spectrum with 10 GeV$\lesssim E_\gamma \lesssim$ 300 GeV has been largely unexplored. Ground-based detectors, such as the Whipple 10m telescope, have large effective areas, but have traditionally been limited to energies above $\sim$300 GeV. Space-based detectors, such as the Energetic Gamma Ray Experiment Telescope (EGRET), have been sensitive to photon energies up to $\sim$20 GeV, but are limited above this energy by their small effective area. There has therefore been an unexplored gap at intermediate energies, which happens to overlap substantially with the range of energies most favored by supersymmetric dark matter.
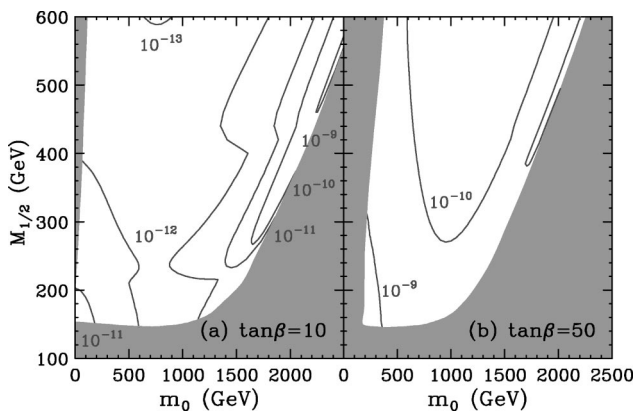

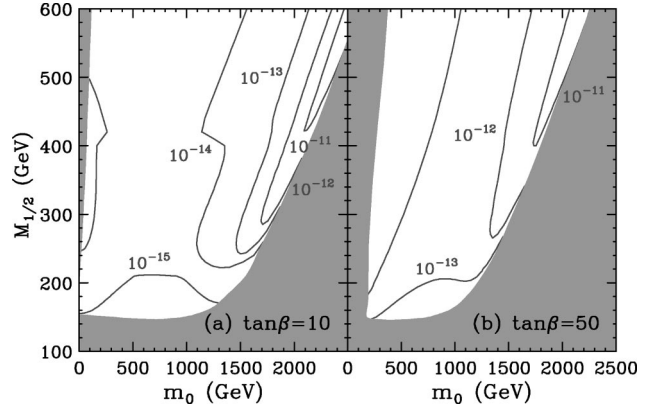FIG. 12. As in Fig. 11, but for the photon energy threshold $E_{thr}=10$ GeV.

FIG. 13. As in Fig. 11, but for the photon energy threshold $E_{thr}=50$ GeV.

The experimental situation is changing rapidly, however. Currently, two heliostat arrays, STACEE and CELESTE, are running with sensitivity in the range 20 GeV$\lesssim E_\gamma \lesssim$ 300 GeV, and many more experiments with greatly improved sensitivity are expected in the next few years. Upcoming experiments with sensitivity to γ rays with 10 GeV$\lesssim E_\gamma$ $\lesssim$ 300 GeV are listed in Table II.

An important figure of merit for the detection of γ rays from the galactic center is the point source flux sensitivity. A compilation of previous estimates of flux sensitivities is given in Fig. 14 for EGRET, STACEE, CELESTE, ARGO-YBJ, MAGIC, AGILE, HESS [99], AMS/γ [95], VERITAS [97], and GLAST [98]. The flux sensitivities for the first six experiments are from Ref. [93], and those for the remaining experiments are from the references listed. The sensitivity of MAGIC assumes the availability of high quantum efficiency photosensors. The sensitivity for CANGAROO III is currently being re-evaluated [100]. We have included it in accord with expectations that it will be comparable to that of HESS. The point flux sensitivities are, of course, dependent

TABLE II. Some of the current and planned γ ray detector experiments with sensitivity to photon energies 10 GeV$\lesssim E_\gamma$ $\lesssim$ 300 GeV. We list each experiment's (proposed) start date and expected E_γ coverage in GeV. The energy ranges are approximate. For experiments constructed in stages, the listed threshold energies will not be realized initially. See the references for details.

| Experiment	Type	Date	E_γ Range
EGRET [88]	Satellite	1991-2000	0.02–30
STACEE [89]	ACT array	1998	20–300
CELESTE [90]	ACT array	1998	20–300
ARGO-YBJ [91]	Air shower	2001	100–2000
MAGIC [92]	ACT	2001	10–1000
AGILE [93]	Satellite	2002	0.03–50
HESS [94]	ACT array	2002	40–5000
AMS/γ [95]	Space station	2003	0.3–100
CANGAROO III [96]	ACT array	2004	30–50000
VERITAS [97]	ACT array	2005	50–50000
GLAST [98]	Satellite	2005	0.1–300
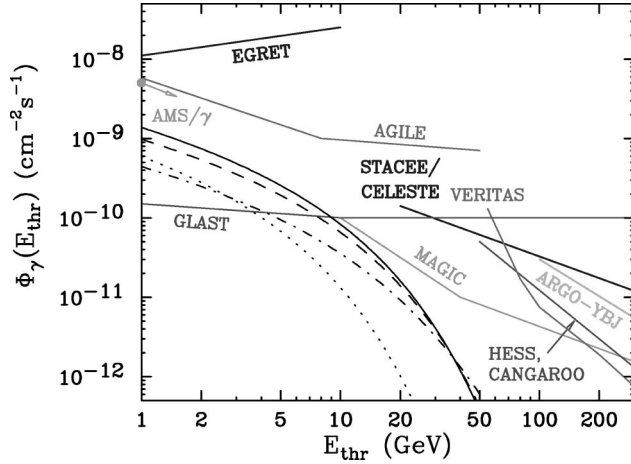
FIG. 14. Integral photon fluxes $\Phi_\gamma(E_{\text{thr}})$ as a function of threshold energy E_{thr} for $A_0 = 0$, $\mu > 0$, $m_t = 174$ GeV, and halo parameter $\bar{J} = 500$. The four models have relic density $\Omega_\chi h^2 \approx 0.15$, and are specified by $(\tan\beta, m_0, M_{1/2}, m_\chi, R_\chi) = (10,100,170,61,0.93)$ (dotted), $(10,1600,270,97,0.77)$ (dashed), $(10,2100,500,202,0.88)$ (dot-dashed), and $(50,1000,300,120,0.96)$ (solid), where all masses are in GeV. Point source flux sensitivity estimates for several gamma ray detectors are also shown. (Care should be taken in comparing these sensitivities to the predicted fluxes—see text.)

on the source's location and energy spectrum. They are also subject to a variety of other experimental uncertainties and assumptions; see the references for details. A typical estimate [97] assumes background extrapolated from EGRET data [88], and a signal distribution $dN_\gamma/dE \propto E^{-2.5}$. Detector efficiencies and cuts are included, and a 5σ signal with at least 10 photons is required. 50 hours of observation is assumed for telescopes, and one year of an all sky survey for the space-based detectors. The arrow for AMS/γ in Fig. 14 indicates that a published estimate exists only for $E_{\text{thr}} = 1$ GeV, but flux sensitivity at some level can be expected out to the detector limit of 100 GeV.

The experimental sensitivities presented clearly cannot be interpreted as future dark matter discovery contours. The neutralino signal has a different energy spectrum than assumed, and the background in the direction of the galactic center is larger, due to the diffuse γ ray emission from the galactic disk [101], which enhances $\sqrt{B}$ by a factor of ~ 5 [102]. (This last fact implies that for some halo profiles, it may be advantageous to center the field of view away from the galactic center. This optimization may significantly reduce potential losses in signal significance.) In addition, there are many ambiguities in background calibration, and, as noted above, the continuum signal is not sufficiently distinct for a simple excess to identify the source as dark matter annihilation. However, the flux sensitivities of Fig. 14 do clearly portend substantial progress in the next few years, and can serve as rough indications of what signal levels will be detectable.

The expected fluxes for four supersymmetry models and $\bar{J} = 500$ are also shown in Fig. 14. Although there is a large uncertainty from halo model dependence, it is clear that detectable signals are possible. At present, EGRET data is

not overly constraining, although halo models with large $\bar{J} \sim 5000$ are within EGRET sensitivity and may even explain a flattening of the spectrum. In the future, AMS/γ and AGILE will improve this sensitivity, and MAGIC may see excesses for $\bar{J} \sim 500$. Finally, GLAST will provide the greatest sensitivity of all, probing halo models with $\bar{J}$ as low as $\bar{J} \sim 50$.

If a significant excess is found in future experiments, its dark matter origin can be tested in a variety of ways. Confirmation from other searches for dark matter or supersymmetry would be the most satisfying possibility. As we will see in Sec. VI, the neutrino and positron signals probe similar models, so a coincidence of various signals is a distinct possibility. However, it has also been suggested that an angular distribution of photons that does not follow the galactic disk and bulge may be a powerful diagnostic [19]. Also, as the dark matter signal has a shape differing from the background, detailed likelihood fits to the photon energy distribution may also be a useful tool, although far beyond the scope of this work. It seems clear, in any case, that for reasonable halo models and supersymmetry parameters, meaningful γ ray signals in the next few years are possible, particularly with gaugino-Higgsino dark matter.

V. POSITRONS

An excess of cosmic anti-particles and anti-matter from dark matter annihilation may be detected in space-based or balloon-borne experiments. The positron signal is perhaps the most promising [103–107]. In the past, soft anti-protons with energies ~ 100 MeV have also been considered [108,109]. However, recent work finds larger background than previously expected, complicating the identification of an anti-proton signal [110,111]. Anti-deuterium has also been suggested as a possibility [112].

The positron background is most likely to be composed of secondaries produced in the interactions of cosmic ray nuclei with interstellar gas, and is expected to fall as $\sim E_{e^+}^{-3.1}$. At energies below 10 GeV, however, this background is subject to large uncertainties from the effects of the solar wind [106,107]. The soft positron spectrum also varies depending on the orbit path of the experiment. At high energies, these effects are negligible. In addition, positrons lose energy through a variety of processes, and so hard ones must typically be produced within a few kpc [106,107]. For this reason, the hard spectrum is relatively insensitive to variations in the halo profile near the galactic center. The dark matter signal is therefore most promising at high energies, where the background is relatively small and well understood.

The differential positron flux is [107]

$$\frac{d\Phi_{e^+}}{d\Omega dE} = \frac{\rho_0^2}{m_\chi^2} \sum_i \sigma_i v B_{e^+}^i \int dE_0 f_i(E_0) \, G(E_0, E), \quad (12)$$

where ρ_0 is the local neutralino mass density, the sum is over all annihilation channels, and $B_{e^+}^i$ is the branching fraction to positrons in channel i. The source function $f_i(E_0)$ gives the initial positron energy distribution from neutralino annihila-

tion. $G(E_0,E)$ is the Green's function describing positron propagation in the galaxy [113] and contains all the halo model dependence.

For the reasons mentioned above, processes yielding hard positrons are by far the most important for dark matter discovery. The "positron line" signal from e^+e^- is helicity-suppressed. It may be enhanced, for example, in the case of B-ino-like LSPs if selectrons are much lighter than all other scalars, but this possibility is highly unmotivated. To an excellent approximation, then, hard positrons arise from $\chi\chi \to WW, ZZ$, followed by the direct decay of gauge bosons to positrons. Assuming unpolarized gauge bosons, f is the familiar flat distribution with endpoints determined by the gauge boson and neutralino masses. The Green's function G has been modeled by Moskalenko and Strong in Ref. [107] in a framework that consistently reproduces a wide range of observational data from anti-protons, nuclei, electrons, positrons, and photons.

Combining all of these results, the differential positron flux may be written as

$$E^2 \frac{d\Phi_{e^+}}{d\Omega dE} = 0.027 \ \mathrm{cm}^{-2} \ \mathrm{s}^{-1} \ \mathrm{sr}^{-1} \ \mathrm{GeV}$$

$$\times \left(\frac{\rho_0}{0.3 \ \mathrm{GeV/cm^3}}\right)^2 \left(\frac{100 \ \mathrm{GeV}}{m_\chi}\right)^2$$

$$\times \sum_i \frac{\sigma_i v}{\mathrm{pb} \cdot \beta_i} B^i_{e^+} \int_{z^i_-}^{z^i_+} dz \, g(z, E/m_\chi), \quad (13)$$

where

$$\beta_{WW,ZZ} = (1 - m^2_{W,Z}/m^2_\chi)^{1/2}, \quad (14)$$

$$z^i_\pm = (1 \pm \beta_i)/2, \quad (15)$$

$$B^{WW}_{e^+} = B(W^+ \to e^+ \nu) = 0.11, \quad (16)$$

$$B^{ZZ}_{e^+} = 2B(Z \to e^+ e^-) = 0.067, \quad (17)$$

and the reduced Green's function is

$$g(z, E/m_\chi) \equiv 10^{a\log^2_{10}E + b\log_{10}E + c} \theta(z - E/m_\chi)$$
$$+ 10^{w\log^2_{10}E + x\log_{10}E + y} \theta(E/m_\chi - z), \quad (18)$$

where E is in GeV and the (z-dependent) coefficients a, b, c and w, x, y are tabulated in Ref. [107] for different halo profiles. As mentioned above, at high energies, these coefficients are fairly independent of the halo model, as high energy positrons originate in our solar neighborhood, where all profiles give similar densities. We adopt coefficients corresponding to the modified isothermal distribution with halo size 4 kpc. For large m_χ, the integral of Eq. (13) is insensitive to m_χ, and so the differential positron flux scales as $\sim 1/m^4_\chi$. Neutralinos with mass not far above m_W are therefore most easily detected.
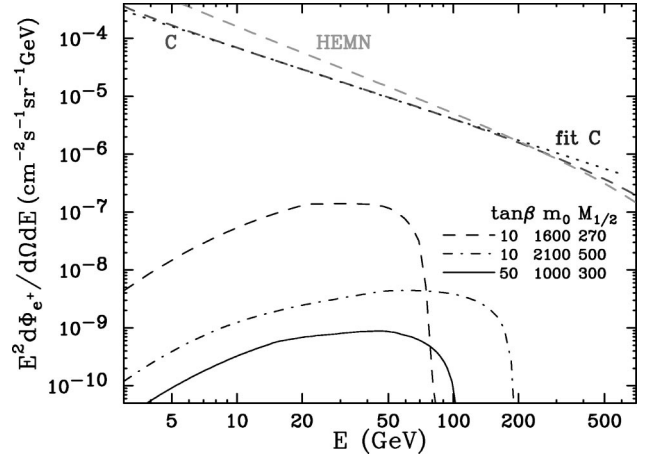

FIG. 15. The differential positron flux for three of the four sample points in Fig. 14. The curves labeled C and HEMN are background models from Ref. [107]; the dotted curve is our fit to C.

In Fig. 15, we show three sample spectra for supersymmetry models yielding relic abundances of $\Omega_\chi h^2 \approx 0.15$. Two background spectra from Ref. [107] are also shown. The signal rates are significantly suppressed relative to those of Refs. [105,107], where the dark matter was assumed to be Higgsino-like. Higgsino-like dark matter is highly disfavored, however, as, unless it is unnaturally heavy, it annihilates too strongly to leave interesting relic abundances. As is evident from Fig. 2, in the allowed minimal supergravity parameter space the LSP is far from pure Higgsino-like, particularly in the region with preferred relic density.

As positrons result from two-body decay, we expect the signal, and the signal to background ratio S/B, to be peaked near $m_\chi/2$. This is evident in the three examples given in Fig. 15. In Fig. 16, we plot the optimal energy E_{opt} at which the signal to background ratio is maximized. Our fit to background C is $E^2 d\Phi_{e^+}/d\Omega dE = 1.16 \times 10^{-3} E^{-1.23}$, where E is in GeV. Comparing with Fig. 1, we see that E_{opt} is indeed approximately $m_\chi/2$ throughout parameter space. In Fig. 17, we plot S/B at E_{opt}. S/B is substantial only in the gaugino-Higgsino region with $m_\chi > m_W$.

Figures 16 and 17 imply that the best experimental hope for indirect detection of dark matter through positrons is in
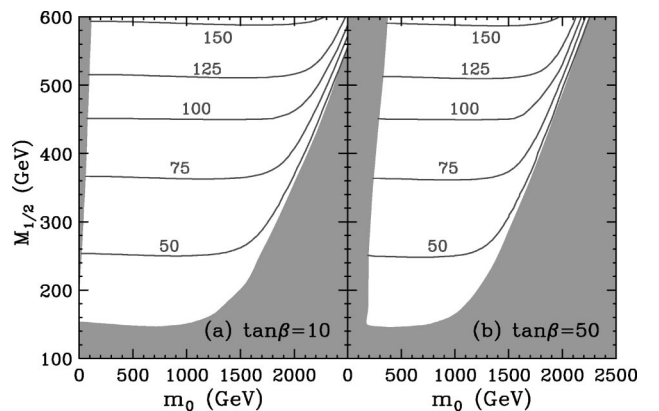

FIG. 16. The optimal positron energy E_{opt} in GeV at which the signal to background ratio S/B is maximized.

experiments sensitive to positron energies above ~ 50 GeV. In the next two to three years, both PAMELA, a satellite detector, and AMS-02, an experiment to be placed on the International Space Station, will satisfy this requirement. These experiments and other recently completed experiments are listed in Table III.

The expected number of positrons per GeV are listed in Table III at positron energies of 50 and 100 GeV. After integrating over some appropriate energy bin size, we see that the expected statistical errors are roughly $\sim 10\%$ for PAMELA, and $\sim 1\%$ for AMS-02. Of course, the signal will also be degraded by systematic errors, particularly in the background calculation. It seems likely, however, that the characteristic peaking of the dark matter signal over an interval of $\mathcal{O}(10$ GeV) will be distinctive. In addition, some systematic errors may be eliminated by considering the ratio $e^+/(e^- + e^+)$. While the positron signal is typically too small for B-ino-like LSPs, an excess of $\sim 1\%$ is possible for gaugino-Higgsino dark matter. The region of detectable positron signals may be extended, however, if, for example, the halo is clumpy, or if the local density is larger than our reference value of 0.3 GeV/cm^3 [106].

VI. COMPARISON WITH OTHER SEARCHES

In the previous three sections, we have examined several indirect signals of neutralino dark matter. As emphasized in Sec. I, however, supersymmetric dark matter cannot exist in isolation, and there are many other avenues for probing supersymmetric models. We now discuss several other promising probes and their projected sensitivities, and we then compare their reaches.

Most closely linked to indirect searches are searches for dark matter scattering off nuclei in low-background detectors. The DAMA Collaboration has reported evidence for an annual modulation signal [118], and the activity in this field will intensify tremendously in the next few years. (For a recent review, see, e.g., Ref. [119].) Here we will use our previous results [6] to estimate the sensitivities of the direct searches. We choose CDMS (Soudan) [120] and CRESST [121] as examples of near-term future experiments. Their projected sensitivities in neutralino-proton cross section are both of order $\sigma_{\mathrm{proton}} \sim 10^{-8}$ pb for 50 GeV $\lesssim m_\chi \lesssim 500$ GeV. More precisely, we parametrize their sensitivities as

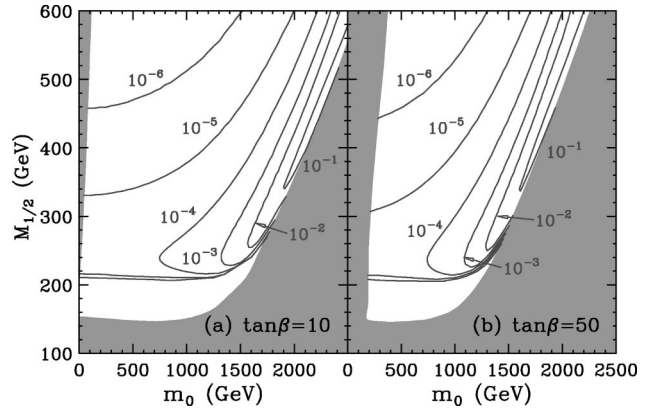FIG. 17. The positron signal to background ratio S/B at E_{opt}.

$$\sigma_{\mathrm{proton}} \simeq \exp\left\{ a + b\left(\frac{m_\chi}{100\ \mathrm{GeV}} \right) + c\left(\frac{m_\chi}{100\ \mathrm{GeV}} \right)^2 \right\}\mathrm{pb},$$

(19)

with $(a,b,c) = (-17, -4.5, 3.1)$ for $m_\chi < 84$ GeV and $(-19, 0.68, -0.057)$ for $m_\chi > 84$ GeV. This limit may be improved by an order of magnitude by the recently proposed GENIUS project [122], or even by CRESST itself, assuming three years of operation with improved background rejection [121].

Among high energy colliders, the Large Hadron Collider (LHC) at CERN is the ultimate supersymmetry discovery machine and will discover at least some superpartners in all of the regions of parameter space we have plotted. The LHC is scheduled to begin operation in its low luminosity mode in 2006. Before that, however, both the LEP II and Tevatron colliders have a chance to discover superpartners. The most stringent constraint from LEP II on minimal supergravity comes from chargino searches. LEP II is now concluding its run, and by the end of 2000 will improve the current chargino mass limits by about 5 GeV. If no signal is seen, this will marginally extend the bottom and right excluded regions of our figures.

The Tevatron will begin operation early in 2001. In the first two years, run IIa will provide an integrated luminosity of 2 fb^{-1} for each detector before a temporary shutdown for a year of detector maintenance and upgrades. In the subsequent run IIb, the data acquisition rate is expected to be

TABLE III. Recent and planned e^+ detector experiments. We list each experiment's (expected) start date, duration, geometrical acceptance in cm^2 sr, maximal E_{e^+} sensitivity in GeV, and (expected) total number of e^+ detected per GeV at $E_{e^+} = 50$ and 100 GeV.

Experiment	Type	Date	Duration	Acceptance	$E_{e^+}^{\mathrm{max}}$	$\frac{dN}{dE}(50)$	$\frac{dN}{dE}(100)$
HEAT94/95 [114]	Balloon	1994/95	29/26hr	495	50	—	—
CAPRICE94/98 [115]	Balloon	1994/98	18/21hr	163	10/30	—	—
PAMELA [116]	Satellite	2002-5	3yr	20	200	7	0.7
AMS-02 [117]	Space station	2003-6	3yr	6500	1000	2300	250

about 5 fb^{-1} per year per detector. Hence, by 2006 we expect $10-12$ fb^{-1} for each Tevatron collaboration. The Tevatron supersymmetry reach has been extensively studied recently [123], with the conclusion that there is some sensitivity, but in rather limited regions of parameter space. The most effective signal is in the clean trilepton channel [124–127] resulting from chargino-neutralino pair production, followed closely by the jets plus E_T channel [128] and the dileptons plus τ jet channel [129]. The maximal reach in chargino mass is 170 GeV in the B-ino LSP region at very low m_0, where the leptonic branching ratios of the electroweak gauginos are enhanced by light sleptons. This degrades rapidly at higher m_0, where hadronic decays are prominent. It also requires moderate $\tan \beta$. At large values of $\tan \beta$, decays to τ leptons dominate the small m_0 region and signatures with τ jets must be used [128,129].

At present there are no dedicated Tevatron studies in the focus point region. (For an LHC study, see Ref. [130].) There are several important modifications to collider signals for $m_0 > 1$ TeV. For example, the lighter chargino and neutralinos are more degenerate, leading to softer decay products, and their branching ratios to b quarks are enhanced by their Higgsino component. Such issues may have a large impact on chargino and neutralino searches at the Tevatron. This is an important question, but currently the Tevatron reach in the focus point region is unknown.

While the Higgs boson is not a supersymmetric particle, supersymmetry (in its economical implementations) restricts its mass, and so Higgs boson searches also have an important impact on supersymmetric models. For LEP II, the ultimate exclusion limit, barring a discovery, is expected to be $m_h > 115$ GeV. At the Tevatron, the 3σ (5σ) Higgs boson discovery reach for 10 fb^{-1} is $m_h \lesssim 100$ (120) GeV [131–133]. The Higgs boson mass, unlike all other quantities investigated here, is sensitive to the A_0 parameter. As the Higgs boson mass limit rises, models with non-zero A_0, large $\tan \beta$, and $m_0 \gtrsim 1$ TeV are increasingly favored [22]. However, for natural values of A_0 [22], 100 GeV$< m_h <$120 GeV and so the Higgs boson will be discovered at the Tevatron at 3σ, but never at 5σ.

Finally, there are many opportunities for discovering supersymmetry in low energy experiments. These include effects in hadronic and leptonic flavor violation, CP violation, proton decay, and electric and magnetic dipole moments. These are discussed more completely in Ref. [24]. Here we will focus on two particularly robust probes: $B \to X_s \gamma$ and the anomalous magnetic moment of the muon.

The best current measurements of $B \to X_s \gamma$ from CLEO and ALEPH can be combined in a weighted average of $B(B \to X_s \gamma)_{\mathrm{exp}} = (3.14 \pm 0.48) \times 10^{-4}$ [134]. These measurements will be improved at the B factories, where large samples of B mesons will greatly reduce statistical errors. However, the uncertainty in the theoretical prediction of the standard model, $B(B \to X_s \gamma)_{\mathrm{SM}} = (3.29 \pm 0.30) \times 10^{-4}$, is likely to remain unchanged. By 2006, a conservative estimate is that both theoretical and experimental uncertainties will be $\sim 0.3 \times 10^{-4}$. Combining them linearly, the 2σ limit will be $2.1 \times 10^{-4} < B(B \to X_s \gamma) < 4.5 \times 10^{-4}$.

The supersymmetric contribution to the muon magnetic dipole moment (MDM) $a_\mu = \frac{1}{2}(g-2)_\mu$ is also a robust probe, since it involves only a few (flavor- and CP-conserving) parameters [135]. The world average is $a_\mu^{\mathrm{exp}} = (116\ 592\ 05 \pm 45) \times 10^{-10}$ [136] and is consistent with the standard model. However, once data currently being taken is analyzed, the Brookhaven experiment E821 is expected to reduce the uncertainty to $\Delta a_\mu \sim 4 \times 10^{-10}$ [137]. At present, uncertainties in the standard model prediction are substantial. Assuming these can be reduced, however, a reasonable estimate for future 2σ sensitivity is $a_\mu^{\mathrm{SUSY}} = 8 \times 10^{-10}$.

In Table IV we present our estimates for sensitivities that will be achieved before the LHC begins operation. The experiments likely to achieve these projections are also listed. Using these estimates, the reach in minimal supergravity parameter space for each mode is given in Figs. 18 and 19. In reading these figures, recall that we have assumed constant local densities in our assessment of dark matter search reaches. If one assumes that the local density is modulated by the thermal relic density, the dark matter reaches outside the shaded regions should be suitably diminished. Within the shaded regions, however, our analysis applies without modification.

Several striking features emerge from Figs. 18 and 19. First, we see that, within the minimal supergravity frame-

TABLE IV. Constraints on supersymmetric models used in Figs. 18 and 19. We also list experiments likely to reach these sensitivities before 2006.

| Observable	Type	Bound	Experiment(s)
$\tilde{\chi}^+ \tilde{\chi}^-$	Collider	$m_{\tilde{\chi}^\pm} > 100$ GeV	LEP: ALEPH, DELPHI, L3, OPAL
$\tilde{\chi}^\pm \tilde{\chi}^0$	Collider	See Refs. [124,127,129]	Tevatron: CDF, D0
$B \to X_s \gamma$	Low energy	$|\Delta B(B \to X_s \gamma)| < 1.2 \times 10^{-4}$	BaBar, BELLE
Muon MDM	Low energy	$|a_\mu^{\mathrm{SUSY}}| < 8 \times 10^{-10}$	Brookhaven E821
σ_{proton}	Direct DM	Eq. (19)	CDMS, CRESST, GENIUS
ν from Earth	Indirect DM	$\Phi_\mu^\oplus < 100$ km^{-2} yr^{-1}	AMANDA, NESTOR, ANTARES
ν from Sun	Indirect DM	$\Phi_\mu^\odot < 100$ km^{-2} yr^{-1}	AMANDA, NESTOR, ANTARES
γ (gal. center)	Indirect DM	$\Phi_\gamma(1) < 1.5 \times 10^{-10}$ cm^{-2} s^{-1}	GLAST
γ (gal. center)	Indirect DM	$\Phi_\gamma(50) < 7 \times 10^{-12}$ cm^{-2} s^{-1}	MAGIC
e^+ cosmic rays	Indirect DM	$(S/B)_{\mathrm{max}} < 0.01$	AMS-02
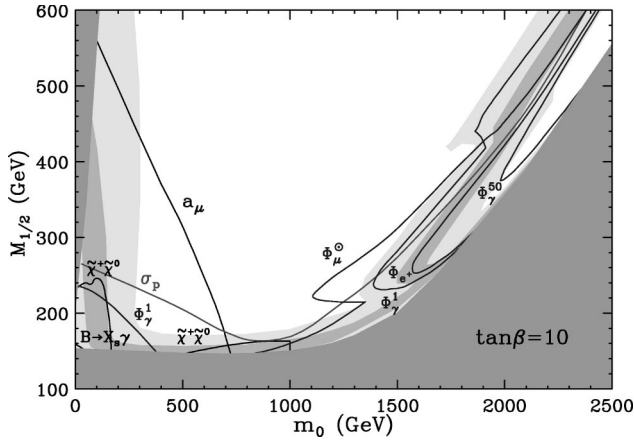
FIG. 18. Estimated reaches of various high-energy collider and low-energy precision searches (black), direct dark matter searches (red), and indirect dark matter searches (blue) before the LHC begins operation, for $\tan\beta=10$. The projected sensitivities used are given in Table IV. (The LEP chargino mass bound will marginally extend the bottom and right excluded regions and is omitted.) The shaded regions are as in Fig. 1. The regions probed extend the curves toward the forbidden, green regions. The dark matter reaches are *not* modulated by the thermal relic density. Bounds from photons from the galactic center are highly halo model-dependent; we assume a moderate halo profile parameter $\bar{J}=500$. (See text.)

work, nearly all of the cosmologically preferred models will be probed by at least one experiment. This is strictly true for $\tan\beta=10$. For $\tan\beta=50$, some of the preferred region escapes all probes, but this requires $M_{1/2}\gtrsim450$ GeV and $m_0\gtrsim1.5$ TeV, and requires significant fine-tuning of the electroweak scale. In the most natural regions, all models in which neutralinos form a significant fraction of dark matter will yield some signal before the LHC begins operation.

Also noteworthy is the complementarity of traditional particle physics searches and indirect dark matter searches. Collider searches require, of course, light superpartners. High precision probes at low energy also require light superpartners, as the virtual effects of superpartners quickly decouple as they become heavy. Thus, the LEP and Tevatron
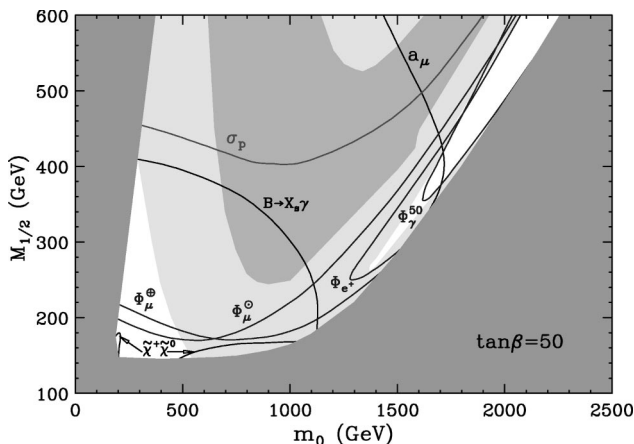

FIG. 19. As in Fig. 18, but for $\tan\beta=50$. Here the Φ_γ^1 probe is sensitive to all of the parameter space shown and so its limit contour does not appear.
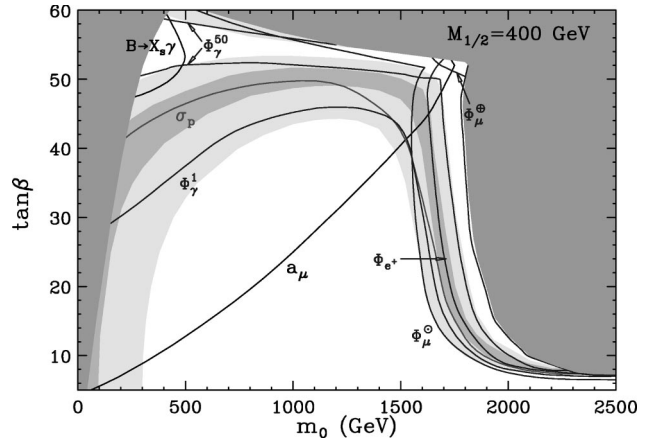

FIG. 20. As in Fig. 18, but in the $(m_0,\tan\beta)$ plane for fixed $M_{1/2}=400$ GeV, $A_0=0$, and $\mu>0$. The regions probed are toward the green regions, except for Φ_γ^{50}, where it is between the two contours. The top excluded region is forbidden by limits on the CP-odd Higgs scalar mass.

reaches are confined to the lower left-hand corner, as are, to a lesser extent, the searches for deviations in $B\to X_s\gamma$ and a_μ. These bounds, and all others of this type, are easily satisfied in the focus point models with large m_0, and indeed this is one of the virtues of these models. However, in the focus point models, *all* of the indirect searches are maximally sensitive, as the dark matter contains a significant Higgsino component. Direct dark matter probes share features with both traditional and indirect searches, and have sensitivity in both regions. It is only by combining all of these experiments, that the preferred region may be completely explored.[4]

Finally, these results have implications for future colliders. In the cosmologically preferred regions of parameter space with $0.1<\Omega_\chi h^2<0.3$, all models with charginos or sleptons lighter than 300 GeV will produce observable signals in at least one experiment. This is evident for $\tan\beta=10$ and 50 in Figs. 18 and 19. In Fig. 20, we vary $\tan\beta$, fixing $M_{1/2}$ to 400 GeV, which roughly corresponds to 300 GeV charginos. We see that the preferred region is probed for any choice of $\tan\beta$. (For extremely low $\tan\beta$ and m_0, there appears to be a region that is not probed. However, this is excluded by current Higgs boson mass limits for $A_0=0$. These limits might be evaded if A_0 is also tuned to some extreme value, but in this case, top squark searches in run II of the Tevatron will provide an additional constraint.)

These results imply that if any superpartners are to be within reach of a 500 GeV lepton collider, some hint of supersymmetry must be seen before the LHC begins collecting data. This conclusion is independent of naturalness considerations. While our quantitative analysis is confined to

---

[4]Note that the complementarity referred to here is not the commonly recognized one, which concerns the mass of the neutralino. It is well-known that some indirect searches are effective even for LSP masses in the TeV range, well beyond the range of colliders. However, such models are highly unnatural, and they have not been considered here.

minimal supergravity, we expect this result to be valid more generally. For moderate values of $\tan\beta$, if the dark matter is made up of neutralinos, they must either be light, B-ino-like, or a gaugino-Higgsino mixture. If they are light, charginos will be discovered. If they are B-ino-like, light sfermions are required to mediate their annihilation, and there will be anomalies in low energy precision measurements. And if they are a gaugino-Higgsino mixture, at least one indirect dark matter search will see a signal. For large $\tan\beta$, low energy probes become much more effective and again there is sensitivity to all probe superpartner spectra with light superpartners. Thus it appears, on qualitative grounds, that all models in which the scalar masses are not widely separated, and the charginos are not extravagantly heavy, will be accessible prior to LHC operation.

VII. CONCLUSIONS

In this paper, we have examined a wide variety of indirect dark matter detection signals. These include neutrinos from annihilation of dark matter in the cores of the Earth and Sun, continuum gamma rays from annihilation in the galactic center, and positron excesses in cosmic rays from annihilation in the local solar neighborhood. In each case, the experimental landscape will be transformed in the next few years by experiments that are running or being mounted. We have tabulated the salient features and reaches of some of the most promising experiments in the previous sections.

We have evaluated the prospects for dark matter detection in the framework of minimal supergravity. This framework incorporates many of the most compelling features of supersymmetry. Previously, this framework has been thought to predict a B-ino-like LSP. That severely limited its utility for dark matter studies. However, recent work has made it clear that gaugino-Higgsino mixtures and even Higgsino-like LSPs are also quite naturally realized in minimal supergravity. We have been careful to include the full range of possibilities, with important (and positive) implications for future dark matter searches.

Let us note in passing that in our parametrization of experimental probes, the case of no-scale supergravity [138], recently revived in the context of gaugino-mediated supersymmetry breaking [139–142], can be regarded as the special case $m_0=0$. Experimental probes of these models are simply evaluated by restricting to the $m_0=0$ axis. Several experiments, notably the trilepton Tevatron search, direct dark matter searches, and Brookhaven experiment E821 will have the power to confirm or exclude this possibility in the near future.

We have concentrated here on discovery signals. If a signal is confirmed, precision measurements may allow experiments to determine dark matter properties. For example, as has been noted in the literature, the neutralino's mass may be determined by the angular spread of the signal in neutrino telescopes. The energy spectrum of gamma rays or positrons signals may provide similar information. The gaugino-ness may also be constrained; indeed, the existence of a significant signal in itself would constitute evidence in favor of mixed gaugino-Higgsinos.

The simplicity of minimal supergravity allows us to compare the reaches of a great variety of probes. We summarize by collecting several of our main conclusions:

B-ino-like dark matter leads to suppressed rates for all indirect dark matter signals. In this case, unless the neutralino is extremely light (near current bounds), all indirect signals are beyond detection for the foreseeable future.

Higgsino-like dark matter cannot yield cosmologically interesting relic densities in a straightforward way. Studies that assume Higgsino-like dark matter exaggerate the power of indirect searches.

Mixed gaugino-Higgsino dark matter gives both relic densities in the preferred range $0.1 \lesssim \Omega_\chi h^2 \lesssim 0.3$ and detectable signals. Such dark matter is naturally present in focus point models, which are favored by low-energy constraints.

Experiments that are running or underway will transform the prospects for indirect dark matter detection. Among the most promising experiments are the neutrino telescopes AMANDA, NESTOR, and ANTARES; the gamma ray telescope MAGIC, and the satellite detector GLAST; and AMS-02, the antiparticle-antimatter search aboard the International Space Station. For mixed gaugino-Higgsino dark matter, these experiments will be sensitive to nearly all models with cosmologically interesting neutralino relic densities, and are competitive with next-generation direct search experiments, such as CDMS (Soudan) and CRESST.

The various indirect searches rely on different sources of neutralino annihilation (cores of the Earth or Sun, galactic center, local solar neighborhood) and so are sensitive to different assumptions. In addition, some signals, particularly the continuum photons, will be difficult to identify unambiguously as a dark matter signal. Without actual data and detailed analyses, it is difficult to make a more precise statement. However, we have seen that many experiments are sensitive to the same supersymmetric models, and given the underlying uncertainties, redundancy is clearly a virtue.

Indirect searches are complementary to traditional particle searches. Separately they probe only portions of the cosmologically preferred model space. Combined, essentially all cosmologically preferred models will produce at least a hint of a signal in one of these experiments *before* the LHC begins operation.

In minimal supergravity models with $0.1 < \Omega_\chi h^2 < 0.3$, *if there is no hint of supersymmetry before the LHC begins operation, no superpartners will be within reach of a 500 GeV lepton collider*. Our arguments are independent of naturalness considerations, and their qualitative structure suggests that similar conclusions will remain valid in alternative frameworks.

[1] For a recent review, see J. R. Primack, ''Cosmological Parameters 2000,'' astro-ph/0007187.

[2] K. Freese, B. D. Fields, and D. S. Graff, in Proceedings of the MPA/ESO Workshop on the First Stars, Garching, Germany, 1999, astro-ph/0002058.

[3] H. Goldberg, Phys. Rev. Lett. **50**, 1419 (1983).

[4] J. Ellis, J. S. Hagelin, D. V. Nanopoulos, and M. Srednicki, Phys. Lett. **127B**, 233 (1983).

[5] LEPSUSYWG, ALEPH, DELPHI, L3 and OPAL experiments, Note LEPSUSYWG/99-03.1.

[6] J. L. Feng, K. T. Matchev, and F. Wilczek, Phys. Lett. B **482**, 388 (2000).

[7] For excellent reviews, see, e.g., M. Drees, Pramana, J. Phys. **51**, 87 (1998); F. Halzen, ''Lectures on neutrino astronomy: Theory and experiment,'' astro-ph/9810368; J. Ellis, ''Particles and cosmology: Learning from cosmic rays,'' astro-ph/9911440; L. Bergström, Rep. Prog. Phys. **63**, 793 (2000).

[8] A. E. Faraggi, K. A. Olive, and M. Pospelov, Astropart. Phys. **13**, 31 (2000).

[9] A. Corsetti and P. Nath, ''Gaugino mass nonuniversality and dark matter in SUGRA, strings and D brane models,'' hep-ph/0003186.

[10] G. F. Giudice and E. Roulet, Nucl. Phys. **B316**, 429 (1989).

[11] G. B. Gelmini, P. Gondolo, and E. Roulet, Nucl. Phys. **B351**, 623 (1991).

[12] R. Gandhi, J. L. Lopez, D. V. Nanopoulos, K. Yuan, and A. Zichichi, Phys. Rev. D **49**, 3691 (1994).

[13] E. Diehl, G. L. Kane, C. Kolda, and J. D. Wells, Phys. Rev. D **52**, 4223 (1995).

[14] A. Corsetti and P. Nath, Int. J. Mod. Phys. A **15**, 905 (2000).

[15] S. Dimopoulos, S. Raby, and F. Wilczek, Phys. Rev. D **24**, 1681 (1981).

[16] L. Bergström and P. Gondolo, Astropart. Phys. **5**, 263 (1996).

[17] L. Bergström, J. Edsjö, and P. Gondolo, Phys. Rev. D **55**, 1765 (1997).

[18] L. Bergström, J. Edsjö, and P. Gondolo, Phys. Rev. D **58**, 103519 (1998).

[19] L. Bergström, P. Ullio, and J. H. Buckley, Astropart. Phys. **9**, 137 (1998).

[20] E. A. Baltz, C. Briot, P. Salati, R. Taillet, and J. Silk, Phys. Rev. D **61**, 023514 (2000).

[21] J. L. Feng, K. T. Matchev, and T. Moroi, Phys. Rev. Lett. **84**, 2322 (2000).

[22] J. L. Feng, K. T. Matchev, and T. Moroi, Phys. Rev. D **61**, 075005 (2000).

[23] J. L. Feng, K. T. Matchev, and T. Moroi, in Proceedings of the 7th International Symposium on Particles, Strings and Cosmology (PASCOS 99), Granlibakken, Tahoe City, California, 1999, hep-ph/0003138.

[24] K. Matchev, talk given at PHENO'00, Madison, Wisconsin, 2000; J. Feng, talk given at the Theoretical Institute on SUSY and Higgs 2000, Argonne, 2000; J. L. Feng and K. T. Matchev, ''Focus point supersymmetry: Proton decay, flavor and CP violation, and the Higgs boson mass,'' hep-ph/0011356.

[25] D. M. Pierce, J. A. Bagger, K. Matchev, and R. Zhang, Nucl. Phys. **B491**, 3 (1997).

[26] S. P. Martin and M. T. Vaughn, Phys. Rev. D **50**, 2282

(1994); I. Jack and D. R. Jones, Phys. Lett. B **333**, 372 (1994); Y. Yamada, Phys. Rev. D **50**, 3537 (1994); I. Jack, D. R. Jones, S. P. Martin, M. T. Vaughn, and Y. Yamada, *ibid.* **50**, 5481 (1994).

[27] J. Bagger, K. Matchev, and D. Pierce, Phys. Lett. B **348**, 443 (1995).

[28] S. Mizuta, D. Ng, and M. Yamaguchi, Phys. Lett. B **300**, 96 (1993).

[29] T. Moroi and L. Randall, Nucl. Phys. **B570**, 455 (2000).

[30] R. Barbieri and G. F. Giudice, Nucl. Phys. **B306**, 63 (1988).

[31] M. Carena, M. Olechowski, S. Pokorski, and C. E. Wagner, Nucl. Phys. **B426**, 269 (1994).

[32] S. Mizuta and M. Yamaguchi, Phys. Lett. B **298**, 120 (1993).

[33] J. Ellis, T. Falk, and K. A. Olive, Phys. Lett. B **444**, 367 (1998).

[34] J. Ellis, T. Falk, K. A. Olive, and M. Srednicki, Astropart. Phys. **13**, 181 (2000).

[35] M. E. Gomez, G. Lazarides, and C. Pallis, Phys. Lett. B **487**, 313 (2000).

[36] P. H. Chankowski, J. Ellis, M. Olechowski, and S. Pokorski, Nucl. Phys. **B544**, 39 (1999).

[37] H. Baer and M. Brhlik, Phys. Rev. D **55**, 3201 (1997).

[38] K. Freese, Phys. Lett. **167B**, 295 (1986).

[39] L. M. Krauss, M. Srednicki, and F. Wilczek, Phys. Rev. D **33**, 2079 (1986).

[40] T. K. Gaisser, G. Steigman, and S. Tilav, Phys. Rev. D **34**, 2206 (1986).

[41] A. Gould, J. A. Frieman, and K. Freese, Phys. Rev. D **39**, 1029 (1989).

[42] W. H. Press and D. N. Spergel, Astrophys. J. **296**, 679 (1985).

[43] J. Silk, K. Olive, and M. Srednicki, Phys. Rev. Lett. **55**, 257 (1985).

[44] M. Srednicki, K. A. Olive, and J. Silk, Nucl. Phys. **B279**, 804 (1987).

[45] J. S. Hagelin, K. W. Ng, and K. A. Olive, Phys. Lett. B **180**, 375 (1986).

[46] K. Ng, K. A. Olive, and M. Srednicki, Phys. Lett. B **188**, 138 (1987).

[47] J. Ellis and R. A. Flores, Nucl. Phys. **B307**, 883 (1988).

[48] G. Jungman, M. Kamionkowski, and K. Griest, Phys. Rep. **267**, 195 (1996); http://t8web.lanl.gov/people/jungman/neut-package.html.

[49] L. Bergström, T. Damour, J. Edsjö, L. M. Krauss, and P. Ullio, J. High Energy Phys. **08**, 010 (1999).

[50] A. Gould and S. M. Khairul Alam, ''Can heavy WIMPs be captured by the earth?,'' astro-ph/9911288.

[51] A. Gould, Astrophys. J. **321**, 560 (1987).

[52] A. Gould, Astrophys. J. **321**, 571 (1987).

[53] A. Gould, Astrophys. J. **328**, 919 (1988).

[54] S. Ritz and D. Seckel, Nucl. Phys. **B304**, 877 (1988).

[55] G. Jungman and M. Kamionkowski, Phys. Rev. D **51**, 328 (1995).

[56] M. Kamionkowski, Phys. Rev. D **44**, 3021 (1991).

[57] A. Bottino, V. de Alfaro, N. Fornengo, G. Mignola, and M. Pignone, Phys. Lett. B **265**, 57 (1991).

[58] A. Bottino, N. Fornengo, G. Mignola, and L. Moscoso, Astropart. Phys. **3**, 65 (1995).

[59] V. Berezinsky, A. Bottino, J. Ellis, N. Fornengo, G. Mignola,

and S. Scopel, Astropart. Phys. **5**, 333 (1996).

[60] K. Freese and M. Kamionkowski, Phys. Rev. D **55**, 1771 (1997).

[61] A. Bottino, N. Fornengo, G. Mignola, M. Olechowski, and S. Scopel, Astropart. Phys. **6**, 395 (1997).

[62] A. Bottino, F. Donato, N. Fornengo, and S. Scopel, Astropart. Phys. **10**, 203 (1999).

[63] A. Bottino, F. Donato, N. Fornengo, and S. Scopel, Phys. Rev. D **62**, 056006 (2000).

[64] Proceedings of the 26th International Cosmic Ray Conference (ICRC 99), Salt Lake City, Utah, 1999, http://krusty.physics.utah.edu/ ~icrc1999/proceedings.html.

[65] Baksan Collaboration, S. P. Mikheyev *et al.*, talk given at the 8th International Workshop on Neutrino Telescopes, Venice, Italy, 1999; O. V. Suvorova, talk given at the 2nd International Conference on Physics Beyond the Standard Model: Beyond the Desert 99, Ringberg Castle, Tegernsee, Germany, 1999, hep-ph/9911415.

[66] Kamiokande Collaboration, M. Mori *et al.*, Phys. Rev. D **48**, 5505 (1993).

[67] MACRO Collaboration, M. Ambrosio *et al.*, Phys. Rev. D **60**, 082002 (1999); MACRO Collaboration, T. Montaruli *et al.*, HE.5.1.03 in Ref. [64], hep-ex/9905021.

[68] Super-Kamiokande Collaboration, A. Okada *et al.*, ''Searches for astronomical neutrino sources and WIMPs with Super-Kamiokande,'' astro-ph/0007003.

[69] Baikal Collaboration, V. A. Balkanov *et al.*, in The proceedings of the 6th International Workshop on Topics in Astroparticle and Underground Physics (TAUP 99), Paris, France, 1999, astro-ph/0001151.

[70] AMANDA Collaboration, E. Dalberg *et al.*, HE.5.3.06 in Ref. [64]; AMANDA Collaboration, A. Karle *et al.*, HE.4.2.05 in Ref. [64].

[71] AMANDA Collaboration, C. Spiering *et al.*, talk given at the 8th International Workshop on Neutrino Telescopes, Venice, Italy, 1999, astro-ph/9906205.

[72] NESTOR Collaboration, L. K. Resvanis *et al.*, talk given at the 8th International Workshop on Neutrino Telescopes, Venice, Italy, 1999.

[73] ANTARES Collaboration, J. R. Hubbard *et al.*, HE.6.3.03 in Ref. [64]; ANTARES Collaboration, L. Moscoso *et al.*, HE.6.3.04 in Ref. [64].

[74] L. Bergström, J. Edsjö, and M. Kamionkowski, Astropart. Phys. **7**, 147 (1997).

[75] M. Urban, A. Bouquet, B. Degrange, P. Fleury, J. Kaplan, A. L. Melchior, and E. Pare, Phys. Lett. B **293**, 149 (1992).

[76] V. S. Berezinsky, A. V. Gurevich, and K. P. Zybin, Phys. Lett. B **294**, 221 (1992).

[77] V. Berezinsky, A. Bottino, and G. Mignola, Phys. Lett. B **325**, 136 (1994).

[78] L. Bergström, J. Edsjö, and P. Ullio, Phys. Rev. D **58**, 083507 (1998).

[79] L. Bergström, J. Edsjö, P. Gondolo, and P. Ullio, Phys. Rev. D **59**, 043506 (1999).

[80] P. Gondolo and J. Silk, Phys. Rev. Lett. **83**, 1719 (1999).

[81] L. Bergström and P. Ullio, Nucl. Phys. **B504**, 27 (1997).

[82] Z. Bern, P. Gondolo, and M. Perelstein, Phys. Lett. B **411**, 86 (1997).

[83] P. Ullio and L. Bergström, Phys. Rev. D **57**, 1962 (1998).

[84] V. S. Berezinsky, A. Bottino, and V. de Alfaro, Phys. Lett. B **274**, 122 (1992).

[85] J. F. Navarro, C. S. Frenk, and S. D. White, Astrophys. J. **462**, 563 (1996).

[86] P. Gondolo, Phys. Lett. B **494**, 181 (2000).

[87] H. U. Bengtsson, P. Salati, and J. Silk, Nucl. Phys. **B346**, 129 (1990).

[88] http://cossc.gsfc.nasa.gov/egret.

[89] STACEE Collaboration, M. C. Chantell *et al.*, Nucl. Instrum. Methods Phys. Res. A **408**, 468 (1998); R. Ong, talk at the 6th GeV-TeV Gamma Ray Astrophysics Workshop, Snowbird, Utah, 1999, http://hep.uchicago.edu/~stacee.

[90] CELESTE and CAT Collaborations, M. de Naurois *et al.*, OG.4.3.06 in Ref. [64]; http://wwwcenbg.in2p3.fr/Astroparticule/celeste/e-index.html.

[91] ARGO-YBJ Collaboration, M. Iacovacci *et al.*, Nucl. Phys. B (Proc. Suppl.) **85**, 338 (2000); http://www1.na.infn.it/wsubnucl/cosm/argo/argo.html.

[92] MAGIC Collaboration, M. Martinez *et al.*, OG.4.3.08 in Ref. [64]; http://hegra1.mppmu.mpg.de.

[93] AGILE Collaboration, A. Morselli *et al.*, OG.4.2.06 in Ref. [64]; http://www.ifctr.mi.cnr.it/Agile.

[94] HESS Collaboration, A. Kohnle *et al.*, OG.4.3.13 and OG.4.3.24 in Ref. [64]; http://www-hfm.mpi-hd.mpg.de/HESS.

[95] R. Battiston, M. Biasini, E. Fiandrini, J. Petrakis, and M. H. Salamon, Astropart. Phys. **13**, 51 (2000); R. Battiston, talk given at the 6th GeV-TeV Gamma Ray Astrophysics Workshop, Snowbird, Utah, 1999, astro-ph/9911241.

[96] CANGAROO Collaboration, M. Mori *et al.*, talk given at the 6th GeV-TeV Gamma Ray Astrophysics Workshop, Snowbird, Utah, 1999; http://icrhp9.icrr.u-tokyo.ac.jp.

[97] VERITAS Collaboration, S. M. Bradbury *et al.* OG.4.3.28 in Ref. [64]; astro-ph/9907248; http://earth.physics.purdue.edu/veritas.

[98] GLAST Collaboration, A. Moiseev *et al.*, HE.5.1.02 in Ref. [64]; http://www-glast.stanford.edu.

[99] Werner Hofmann, for the HESS Collaboration, ''The High Energy Stereoscopic System (HESS) Project;'' http://www-hfm.mpi-hd.mpg.de/HESS/public/publications/tevhess.ps.gz.

[100] M. Mori (private communication).

[101] P. Chardonnet, P. Salati, J. Silk, I. Grenier, and G. Smoot, Astrophys. J. **454**, 774 (1995).

[102] EGRET Collaboration, S. D. Hunter *et al.*, Astrophys. J. **481**, 205 (1997).

[103] A. J. Tylka, Phys. Rev. Lett. **63**, 840 (1989).

[104] M. S. Turner and F. Wilczek, Phys. Rev. D **42**, 1001 (1990).

[105] M. Kamionkowski and M. S. Turner, Phys. Rev. D **43**, 1774 (1991).

[106] E. A. Baltz and J. Edsjo, Phys. Rev. D **59**, 023511 (1999).

[107] I. V. Moskalenko and A. W. Strong, Phys. Rev. D **60**, 063003 (1999).

[108] F. W. Stecker and A. J. Tylka, Astrophys. J. Lett. **336**, L51 (1989).

[109] P. Chardonnet, G. Mignola, P. Salati, and R. Taillet, Phys. Lett. B **384**, 161 (1996).

[110] L. Bergström, J. Edsjö, and P. Ullio, ''Cosmic antiprotons as a probe for supersymmetric dark matter?,'' astro-ph/9902012.

[111] J. W. Bieber, R. A. Burger, R. Engel, T. K. Gaisser, S.

Roesler, and T. Stanev, Phys. Rev. Lett. **83**, 674 (1999).

[112] F. Donato, N. Fornengo, and P. Salati, Phys. Rev. D **62**, 043003 (2000).

[113] R. J. Protheroe, Astrophys. J. **254**, 391 (1982).

[114] HEAT Collaboration, S. W. Barwick *et al.*, Phys. Rev. Lett. **75**, 390 (1995); M. A. DuVernois *et al.*, OG.1.1.14 in Ref. [64].

[115] WIZARD-CAPRICE Collaboration, M. Boezio *et al.*, Astrophys. J. **532**, 653 (2000); M. Boezio *et al.*, OG.1.1.16 in Ref. [64]; M. Boezio, Ph.D. thesis, Royal Institute of Technology, Stockholm, Sweden, 1998.

[116] PAMELA Collaboration, OG.4.2.04 in Ref. [64]; http://wizard.roma2.infn.it/pamela/fram_des.htm.

[117] AMS Collaboration, S. Ahlen *et al.*, Nucl. Instrum. Methods Phys. Res. A **350**, 351 (1994); B. Alpat *et al.*, ''The AMS (Alpha Magnetic Spectrometer) Experiment on the International Space Station,'' talk given at the 8th Pisa meeting on Advanced Detectors: Frontier Detectors for Frontier Physics, 2000; http://ams.cern.ch/AMS.

[118] DAMA Collaboration, R. Bernabei *et al.*, Phys. Lett. B **480**, 23 (2000).

[119] L. Baudis and H. V. Klapdor-Kleingrothaus, ''Direct detection of nonbaryonic dark matter,'' astro-ph/0003434.

[120] CDMS Collaboration, R. W. Schnee *et al.*, Phys. Rep. **307**, 283 (1998).

[121] CRESST Collaboration, M. Bravin *et al.*, Astropart. Phys. **12**, 107 (1999).

[122] GENIUS Collaboration, H. V. Klapdor-Kleingrothaus *et al.*, ''GENIUS: A supersensitive germanium detector system for rare events,'' hep-ph/9910205.

[123] SUGRA Working Group Collaboration, S. Abel *et al.*, ''Report of the SUGRA working group for run II of the Tevatron,'' hep-ph/0003154.

[124] K. T. Matchev and D. M. Pierce, Phys. Rev. D **60**, 075004 (1999).

[125] H. Baer, M. Drees, F. Paige, P. Quintana, and X. Tata, Phys. Rev. D **61**, 095007 (2000).

[126] V. Barger and C. Kao, Phys. Rev. D **60**, 115015 (1999).

[127] K. T. Matchev and D. M. Pierce, Phys. Lett. B **467**, 225 (1999).

[128] H. Baer, C. Chen, M. Drees, F. Paige, and X. Tata, Phys. Rev. D **58**, 075008 (1998).

[129] J. D. Lykken and K. T. Matchev, Phys. Rev. D **61**, 015001 (2000); ''Tau jet signals for supersymmetry at the Tevatron,'' hep-ex/9910033.

[130] B. C. Allanach, J. P. Hetherington, M. A. Parker, and B. R. Webber, J. High Energy Phys. **08**, 017 (2000).

[131] Report of the Higgs Working Group, conveners M. Carena, J. Conway, H. Haber, and J. Hobbs, http://fnth37.fnal.gov/higgs.html.

[132] H. Baer, B. W. Harris, and X. Tata, Phys. Rev. D **59**, 015003 (1999).

[133] M. Carena, S. Mrenna, and C. E. Wagner, Phys. Rev. D **60**, 075010 (1999).

[134] A. L. Kagan and M. Neubert, Eur. Phys. J. C **7**, 5 (1999).

[135] T. Moroi, Phys. Rev. D **53**, 6565 (1996).

[136] R. Carey, talk given at the XXXth International Conference on High Energy Physics (ICHEP00), Osaka, Japan, 2000.

[137] E821 Collaboration, M. Grosse Perdekamp *et al.*, Nucl. Phys. B (Proc. Suppl.) **76**, 253 (1999).

[138] A. B. Lahanas and D. V. Nanopoulos, Phys. Rep. **145**, 1 (1987).

[139] D. E. Kaplan, G. D. Kribs, and M. Schmaltz, Phys. Rev. D **62**, 035010 (2000).

[140] Z. Chacko, M. A. Luty, A. E. Nelson, and E. Ponton, J. High Energy Phys. **01**, 003 (2000).

[141] M. Schmaltz and W. Skiba, Phys. Rev. D **62**, 095005 (2000).

[142] M. Schmaltz and W. Skiba, Phys. Rev. D **62**, 095004 (2000).